QSO Catalogue for Gaia
GWP-S-335-13000

Alexandre H. Andrei (Observatório Nacional/MCT, and associated researcher to INAF/Osservatorio Astronomico Turin, SYRTE/Observatoire de Paris and Observatório do Valongo/UFRJ), Christophe Barache (SYRTE/Observatoire de Paris), Dario N. da Silva Neto (UEZO), François Taris (SYRTE/Observatoire de Paris), Geraldine Bourda (Observatoire de Bordeaux), Jean-François Le Campion (Observatoire de Bordeaux), Jean Souchay (SYRTE/Observatoire de Paris), J.J. Pereira Osório (Centro de Investigação em Ciências Geo-Espaciais/FCUP), Júlio I. Bueno de Camargo (Observatório Nacional/MCT), Marcelo Assafin (Observatório do Valongo/UFRJ), Roberto Vieira Martins (Observatório Nacional/MCT), Sébastien Bouquillon (SYRTE/Observatoire de Paris), Sébastien Lambert (SYRTE/Observatoire de Paris), Sonia Anton (Centro de Investigação em Ciências Geo-Espaciais/FCUP and SIM), Patrick Charlot (Observatoire de Bordeaux)

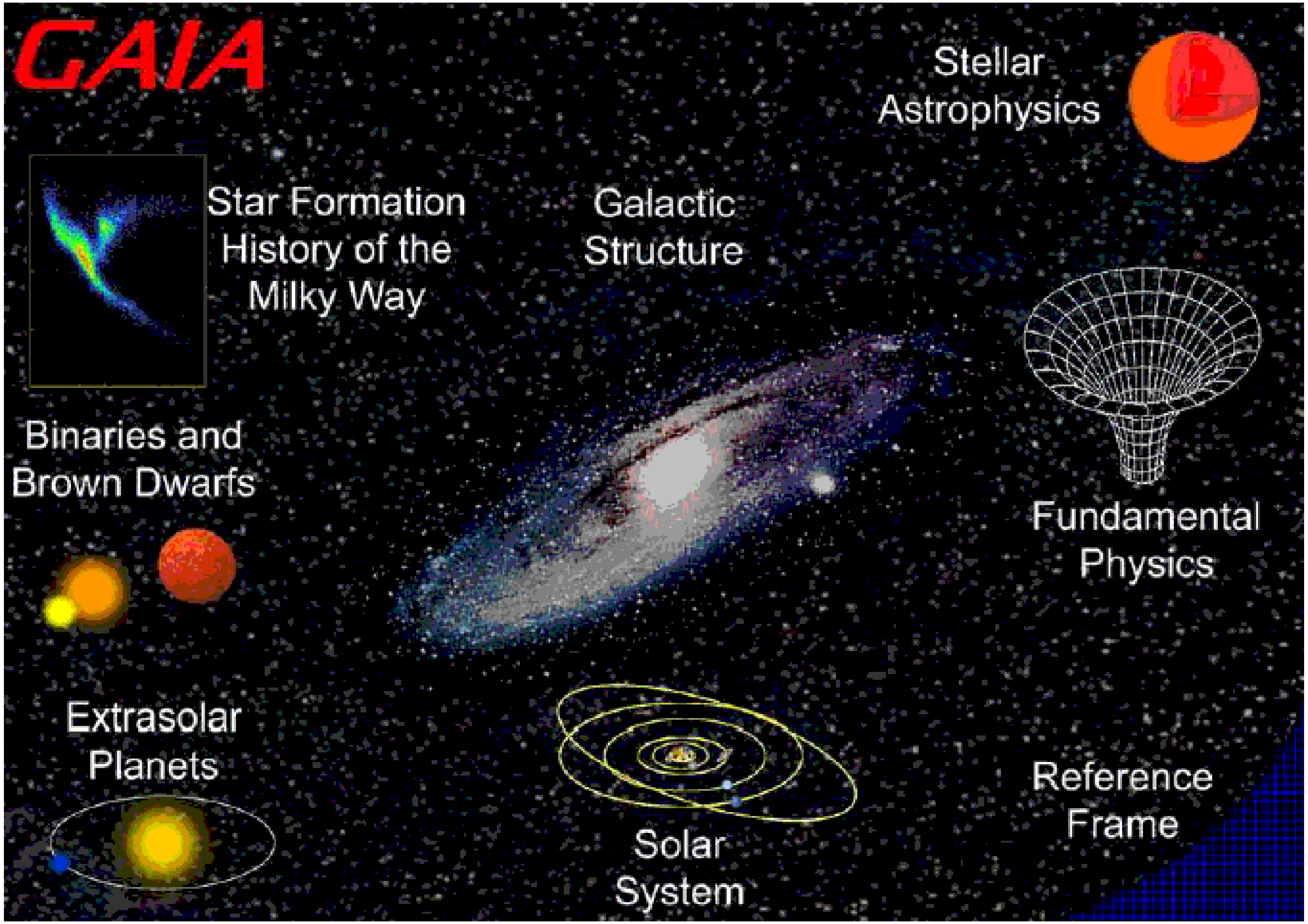
GAIA
Stellar Astrophysics
Star Formation History of the Milky Way
Galactic Structure
Binaries and Brown Dwarfs
Fundamental Physics
Extrasolar Planets
Solar System
Reference Frame

Gaia will perform micro-arcsecond (μas) **global astrometry for all ~1,000 million stars down to G ≈ 20 mag** — except for the ~6,000 brightest stars in the sky — by linking objects with both small and large angular separations in a network in which each object is connected to a large number of other objects in every direction. Over the five-year mission lifetime, a star transits the astrometric instrument on average ~70 times, leading to ~630 CCD transits. Gaia will not exclusively observe stars: *all* objects brighter than G ≈ 20 mag will be observed, including **solar-system objects such as asteroids and Kuiper-belt objects, quasars, supernovae, multiple stars, etc**. The Gaia CCD detectors feature a pixel size of 10 μm (59 milli-arcsecond) and the astrometric instrument has been designed to cope with object densities up to 750,000 stars per square degree. In denser areas, only the brightest stars are observed and the completeness limit will be brighter than 20th magnitude.

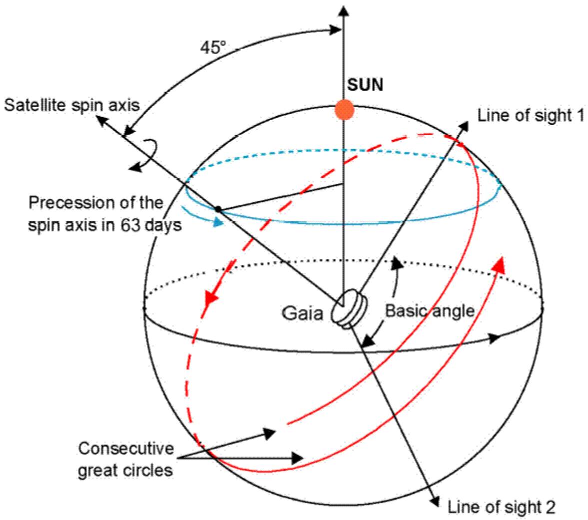

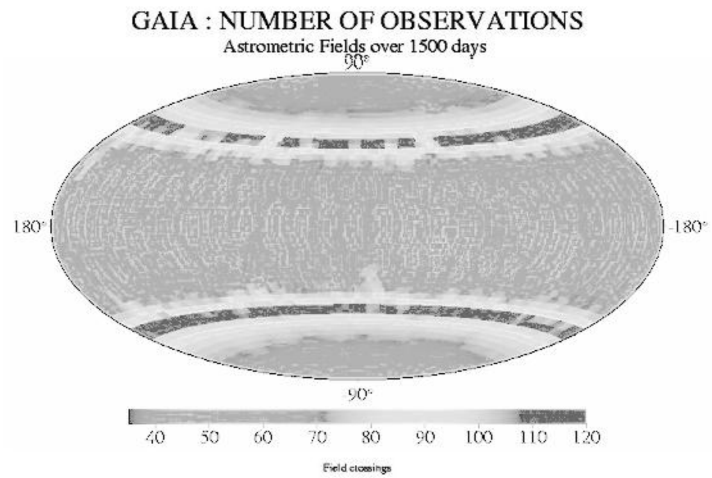

The manifold Gaia scientific output relies on precise astrometry accurate to submas standards.

This depends on building a fundamental reference frame formed by pointlike, position stable, and allsky homogeneous grid points.

In one word, quasars.

The Gaia CU3 Initial Quasar Catalogue Working Package was established to beforehand produce one such list, although ultimately the satellite multiband photometry aided by astrometric monitoring has the potential to pick up a clean sample of quasars.

Quasars in Gaia

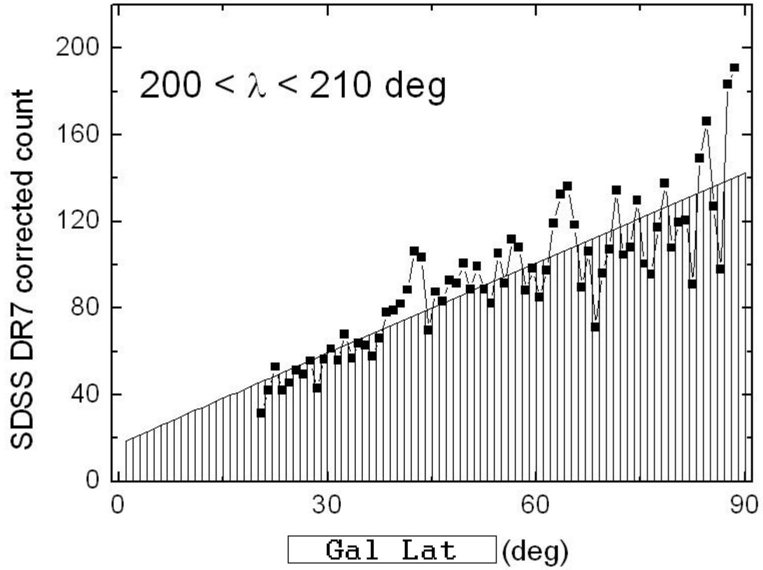

The projected number of QSOs that will be observed by Gaia is ~ 500,000

From ground the number of known QSOs vary from ~ 100,000 to ~ 2,000,000 - depending on the degree of certainty upon its recognition

Current large QSOs databases are
Veron-Cetty & Veron – 13th edition, 2010 – 133,336 QSOs, etc
LQAC/LQRF – 2nd edition, 2011 - 187,504 QSOs (astrometry)
SDSS/DR7 – 5th edition, 2010 - 105,783 QSOs (specttoscopic redshift)
MILLIQUAS – 2.9 edition, 2012 - 1,184,209 objects
and
Gaia Initial Quasar Catalog – GIQC IV - 136,643 well documented quasars, (plus 50,862 candidates)

All of them, either have no homogeneous sky coverage and/or no reliable astrometry at 1arcsec level, and/or no clearly defined photometry standards, and/or no clearly defined morphology and variability assessment, and/or no clearly defined AGN classification.

Quasars in Gaia

That is, also for QSOs the Gaia survey will be unique. Therefore a Gaia self-sufficient QSO recognition scheme is required.

The method of choice is photometric identification
Using of the prism dispersion Blue and Red Photometers images

Led initially by J.F. Claeskens (Univ. of Liège, Belgium)
Then continued by C. Bailer Jones (MPIA, Germany)

Template set from synthetic library covering the full wavelength range sampled by Gaia (λ 2400 – 10 500A°), modeling slope and intensity.

To select a small clean sample of QSOs free of stellar contaminants
To identify the majority of the QSOs in not a so clean sample

Main contaminant: very red (M stars), or highly reddened stars and peculiar white dwarfs

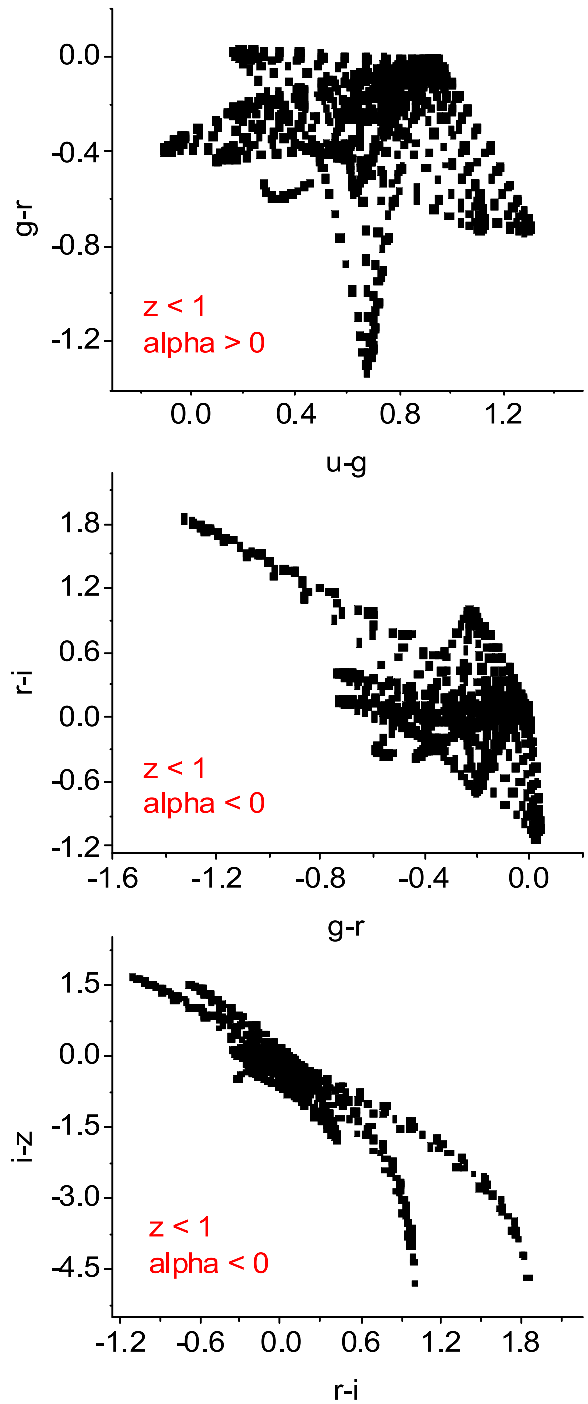

Quasars in Gaia - Probabilistic Classifier

The objects sample completeness is 99% with a contamination of 0.7%.
Including parallax and proper motion in the classifier barely changes the results.

Morphology (host galaxy signature) and variability locus might be also included

Not accounting for class priors in the target population leads to misclassifications and poor predictions for sample completeness and contamination.

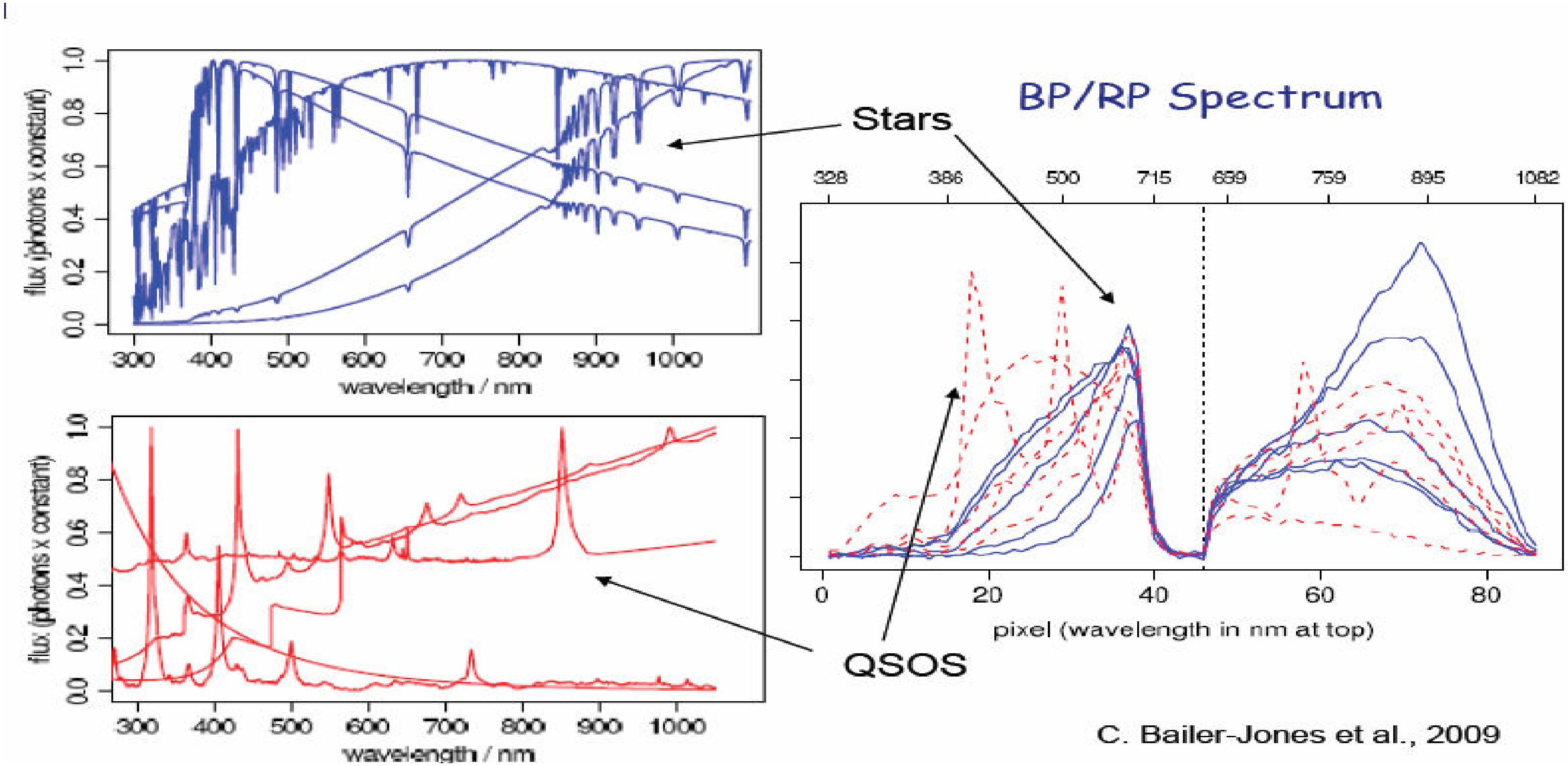

C. Bailer-Jones et al., 2009

The Catalog

Sky Distribution (galactic disk shown) – **1deg^2 cells count**

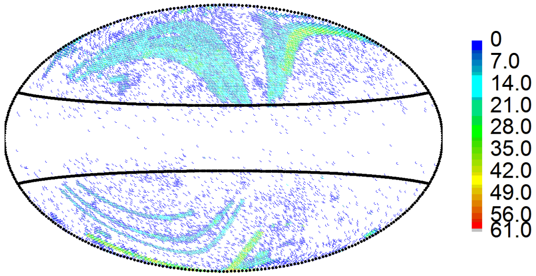

V&V

85,221 sources

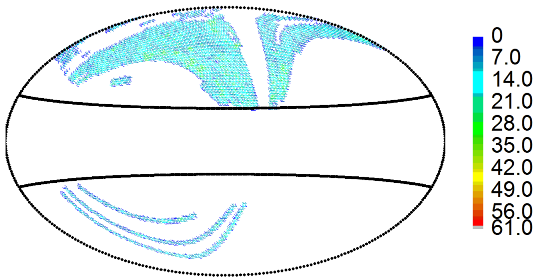

SDSS DR5

74,869 sources

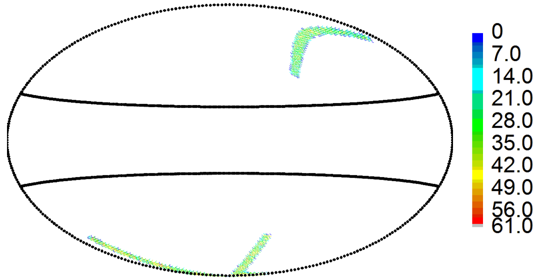

2dF – QSO

23,803 sources

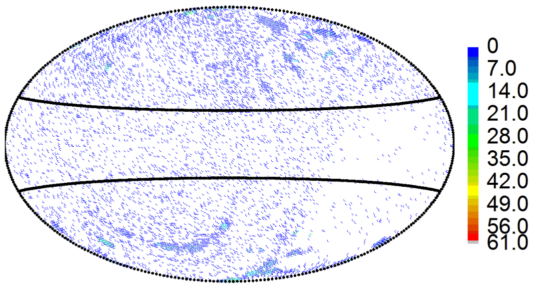

All Radio QSOs

11,781 sources

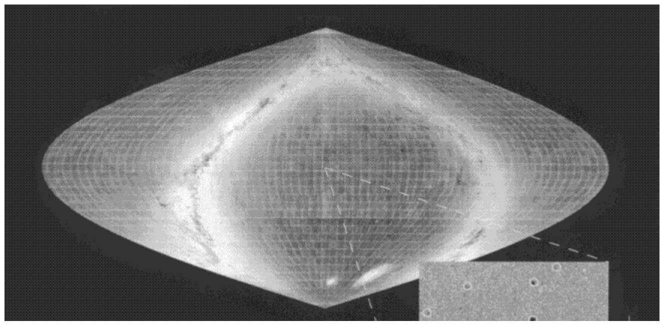

B1.0

All sky up to V=21

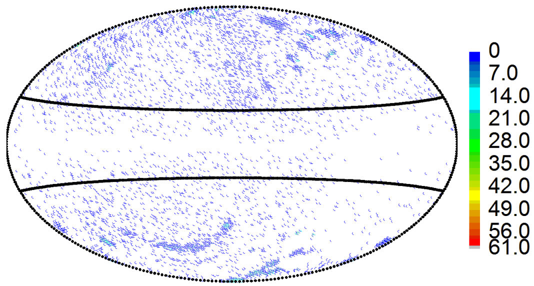

Radio QSOs
found in B1.0

6,941 sources

The Catalog - GIQC I - 2007

Contained 128,257 candidates QSOs. At least one redshift determination for 98.75%, and at least one magnitude determination for 99.20%.

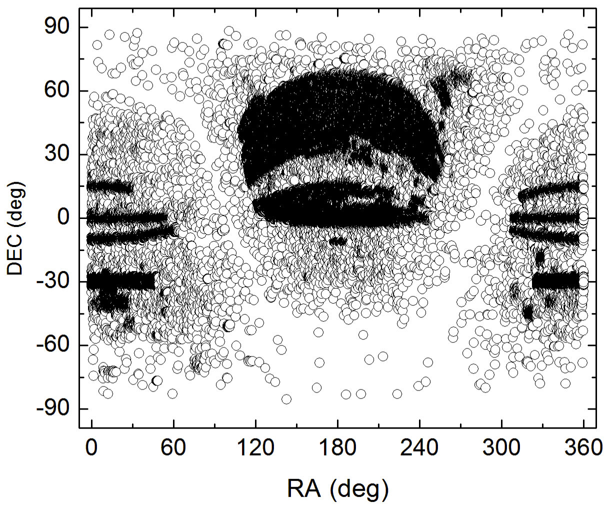

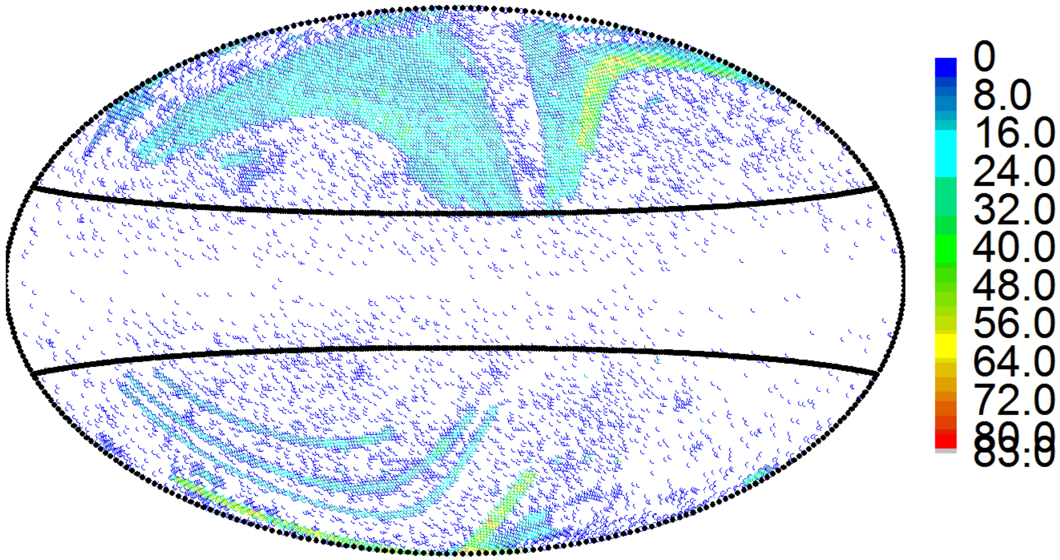

CU3 Task Force (GWP-S-335-13000) - QSO Catalogue for Gaia

Objective: **To obtain a clean sample of at least 10,000 quasars, distributed allsky above |*b*|>|20deg|, with magnitude smaller than V=20 and pointlike PSF.**

The Catalog – LQAC2

Table 2. Number of cross-identified objects between the catalogues belonging to the LQAC

Catalog Name	A	B	C	D	E	F	G	H	I	J	K	L	M
A (ICRF2)	**3414**	3414	1595	1569	423	35	0	70	619	1193	2553	2398	1827
B (VLBA)	-	**5198**	1674	1752	528	39	2	96	678	1598	3362	3144	2163
C (VLA)	-	-	**1858**	1271	301	10	0	54	467	752	1385	1326	1182
D (JVAS)	-	-	-	**2118**	384	6	1	53	317	681	1558	1496	1067
E(SDSS)	-	-	-	-	**126577**	2140	736	773	1877	13442	102866	101322	23494
F (2QZ)	-	-	-	-	-	**23660**	765	0	501	722	22283	21255	22883
G(FIRST)	-	-	-	-	-	-	**9058**	3	58	37	7152	4892	8550
H(2dF-SDSS LRG)	-	-	-	-	-	-	-	**969**	134	628	941	944	958
I(HB)	-	-	-	-	-	-	-	-	**6721**	2411	6654	6480	6299
J(2MASS)	-	-	-	-	-	-	-	-	-	**25252**	24731	24571	14226
K(GSC23)	-	-	-	-	-	-	-	-	-	-	**154900**	145755	54278
L(B1.0)	-	-	-	-	-	-	-	-	-	-	-	**148894**	50633
M(VV2009)	-	-	-	-	-	-	-	-	-	-	-	-	**80667**

The Catalog – Color Space

The distributions approach well to Gaussians, then they can be used to define the QSOs locus (based on B1.0 colors only).

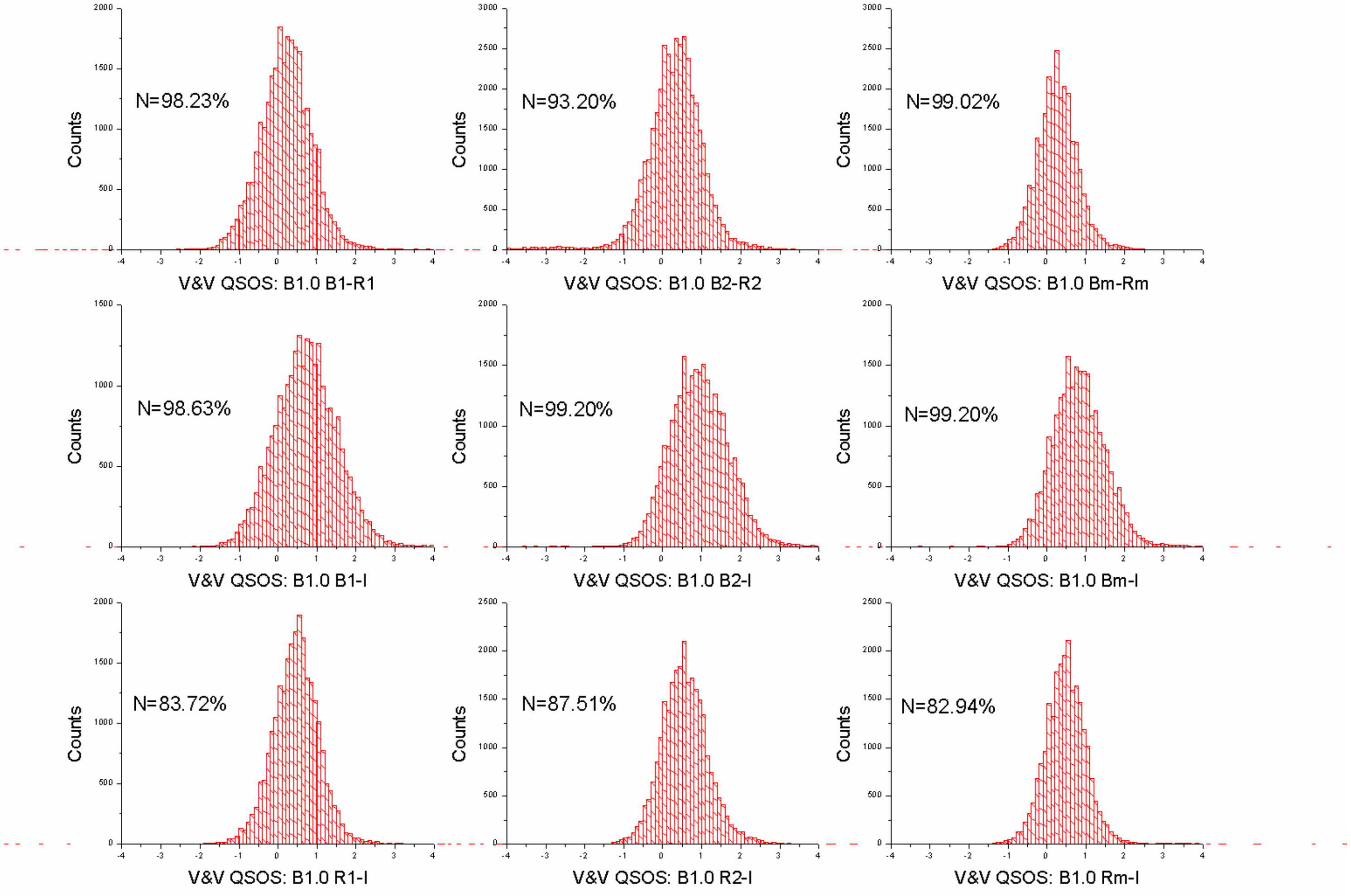

The Catalog – reliability tests

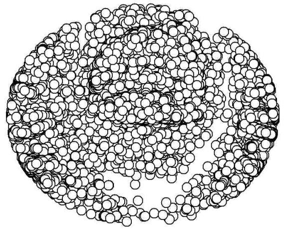

Number of QSOS found in USNO B1.0: 98,920

Are they real ? A fake sample was generated by shifting the GSC23 QSOs sample positions by 5arcmin on right ascension and on declination. The shift is sufficiently small to keep the fake sources in the same neighborhood as the corresponding true ones. A 2arcsec search now results in only 0.1% matches.

- Classification: 94,920 QSOs amidst 58,304,812 stars!
- Scheme: nearest space algorithm
- Results: Best outputs using B-R and B-I colors, Magnitude > 17^{th} R, μ < 5mas/y, μ significance <1
- 1 known QSO out of 10 candidates

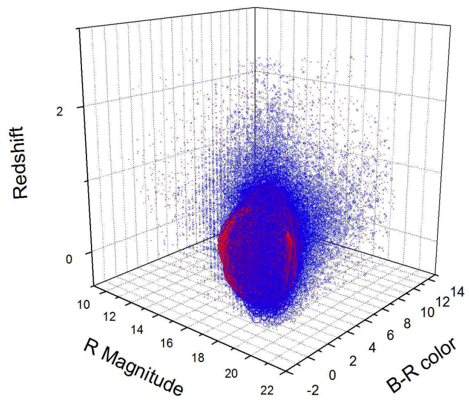

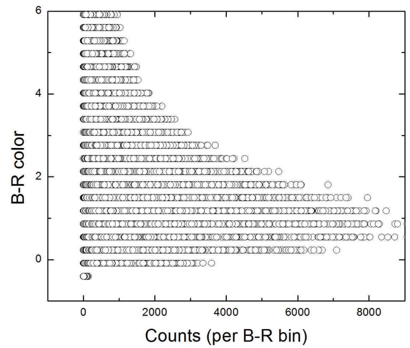

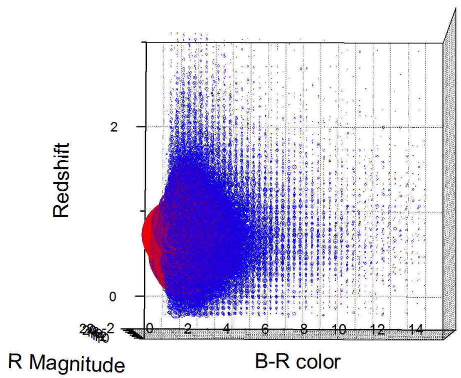

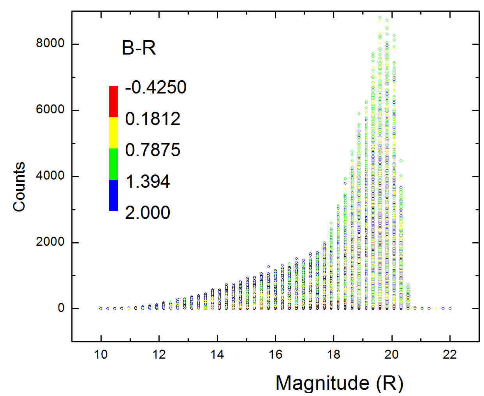

The Catalog – LQRF

Input Optical Catalogues Astrometry

USNO B1.0	GSC 2.3	SDSS DR5

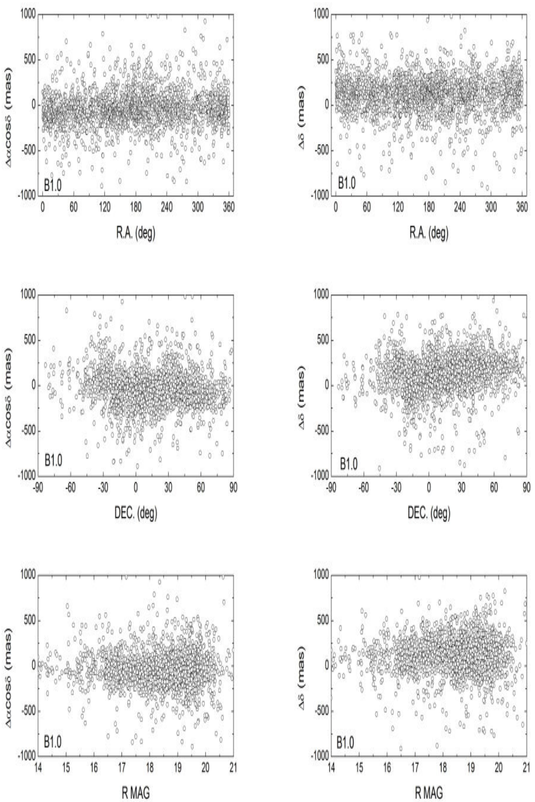

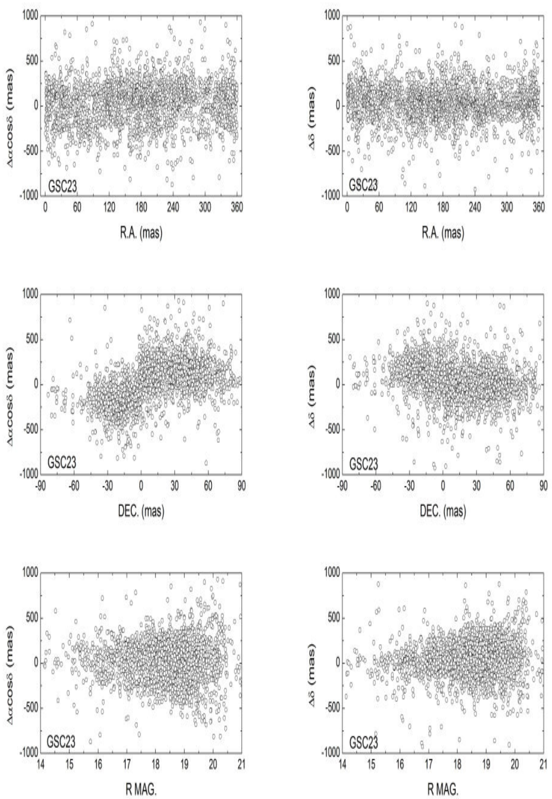

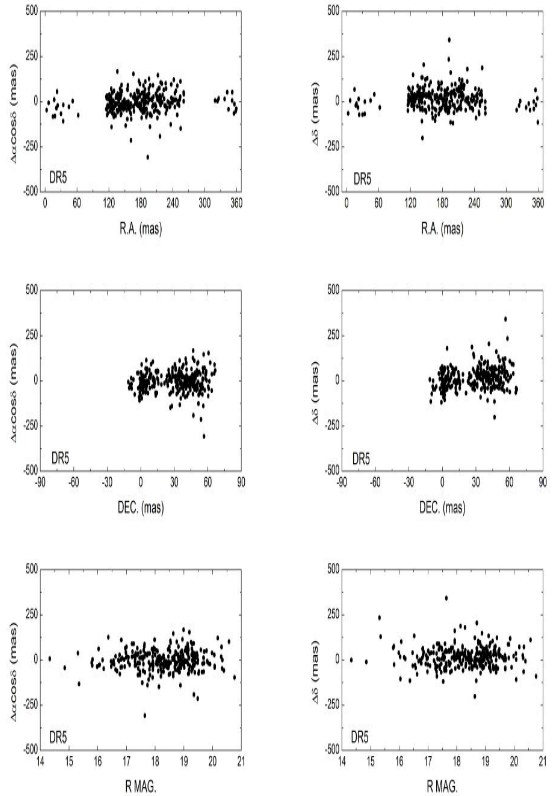

USNO B1.0	GSC 2.3	SDSS DR5
<Δαcosδ>= -37.1±4.7	<Δαcosδ>= +28.3±5.5	<Δαcosδ>= -4.0±3.4
<Δδ> = +120.5±4.9	<Δδ> = +38.5±4.8	<Δδ> = +16.6±3.5

Local Astrometric Correction

- 67”/mm plate scale, small regions, at least 6 reference stars
- 1st degree complete polynomial or 4 constants (low number of stars)
- Reduction by UCAC2 and 2Mass

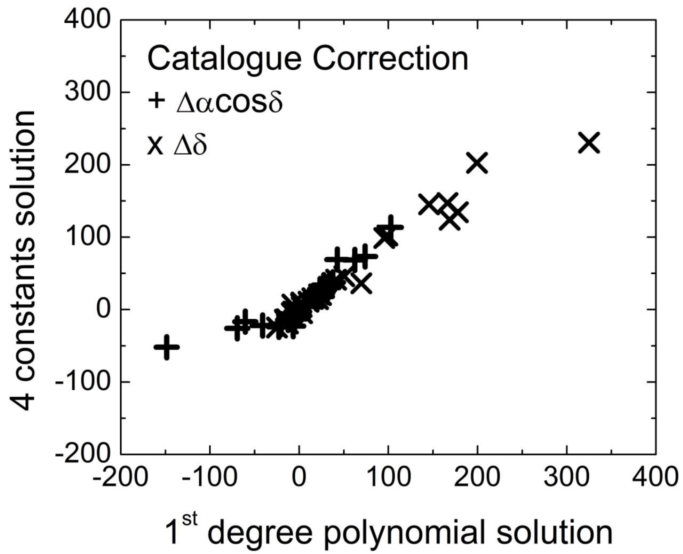

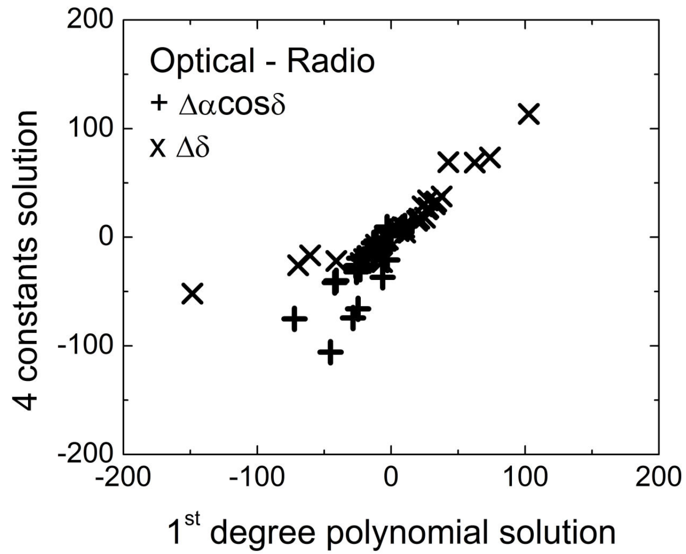

The Catalog – LQRF

Rotation and Equatorial Bias to the ICRF

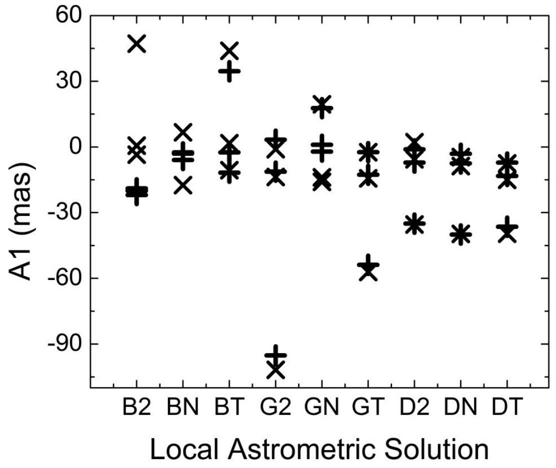

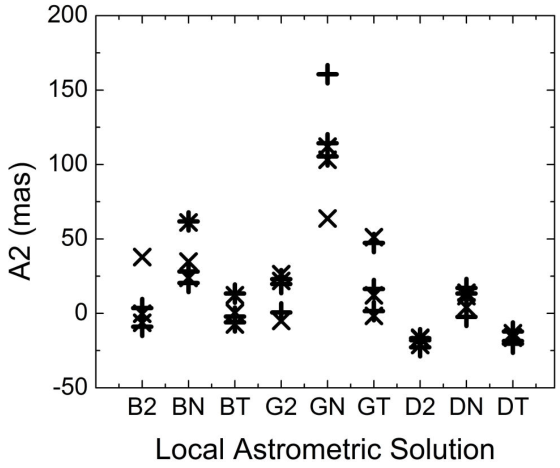

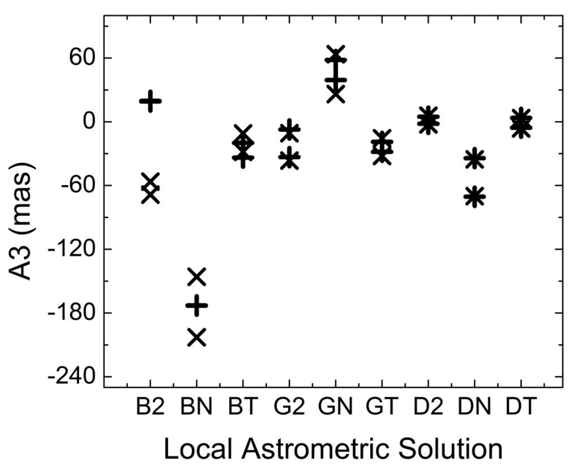

Solution	A1	A2	A3	A4
BU	-3±17	-9±18	-76±13	+15±15
BT	-2±12	-2±14	-33±11	-12±12
GU	-11±13	+19±14	-7±10	+21±12
GT	-12±10	+16±11	-18±9	+0±10
DU	-7±4	-18±4	+4±3	+15±3
DT	-13±5	-18±5	+3±4	+23±4

All values in mas

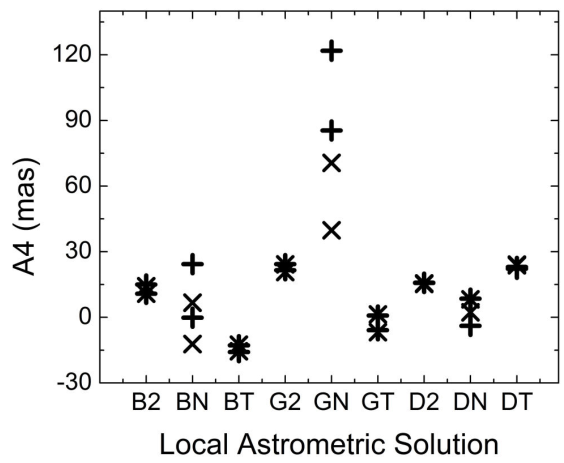

The Catalog – LQRF

Spherical Harmonics

$$\mathbf{Ac = Ccpnml \times Hp(R') \times Ln(\sin\delta) \times Fml(\alpha)}$$

- terms up to 30th order
- 2,760 terms significant to 3σ
- isolated terms are minority (mostly on **δ**)
- progressive solution from lower order terms
- now only 16 significant terms
- magnitude terms significant for the GSC2.3
- Higher order terms for DR5 (mostly relative to UCAC2

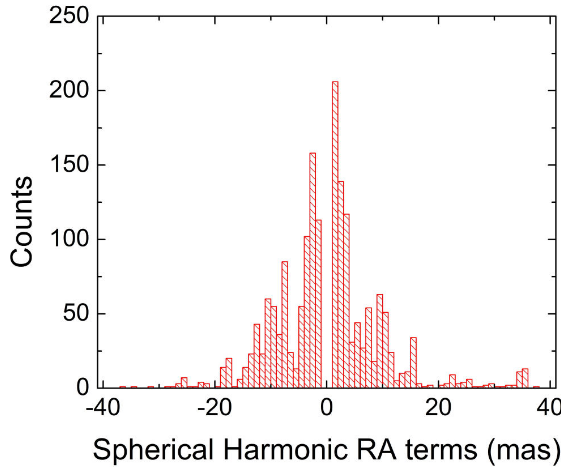

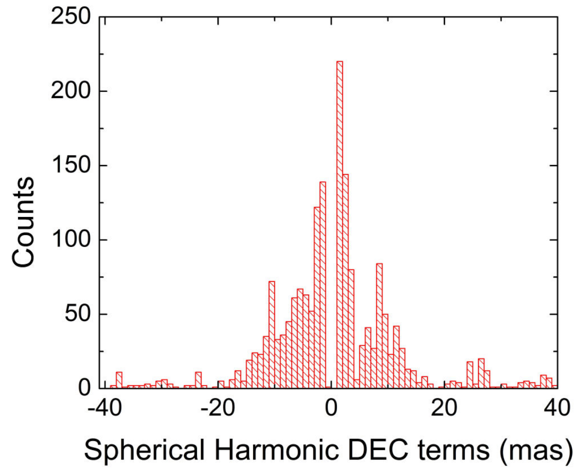

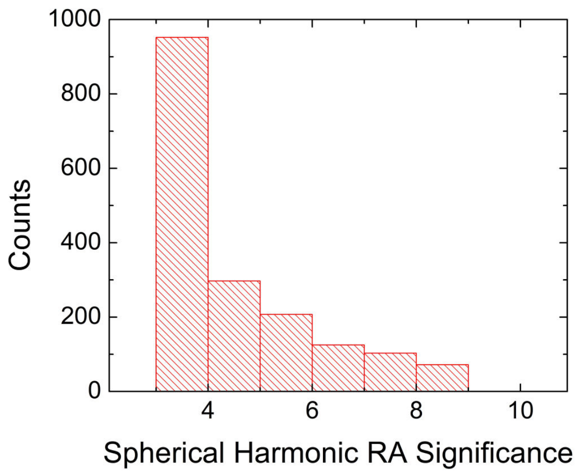

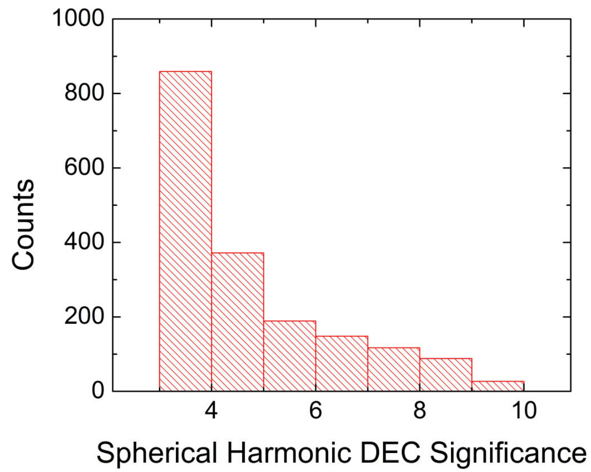

The Catalog - LQRF **-** 100,165 qsos present in at least one available optical image, as recorded in the SDSS DR6, GSC2.3, and USNO B1.0.

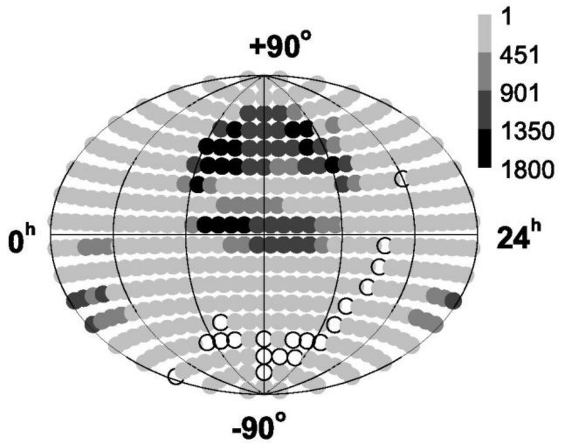

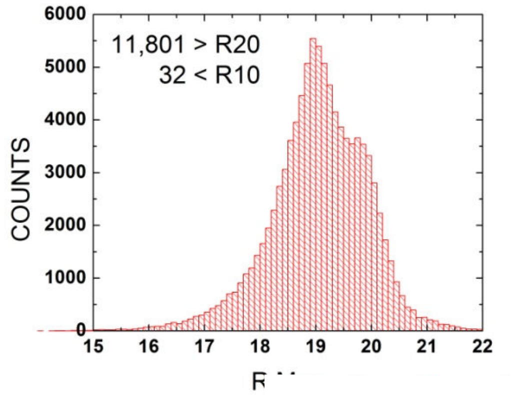

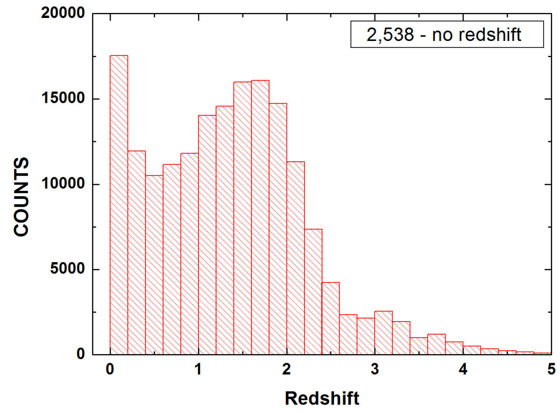

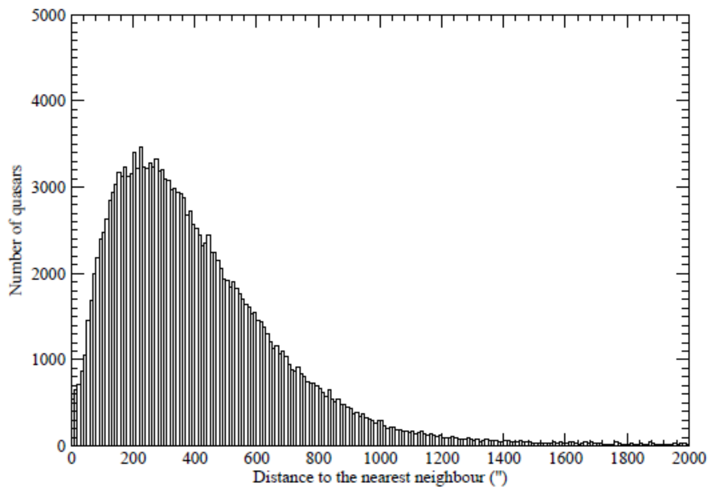

Fig. 10. Histogram of distance to the nearest neighbour for the whole LQAC-2 catalogue.

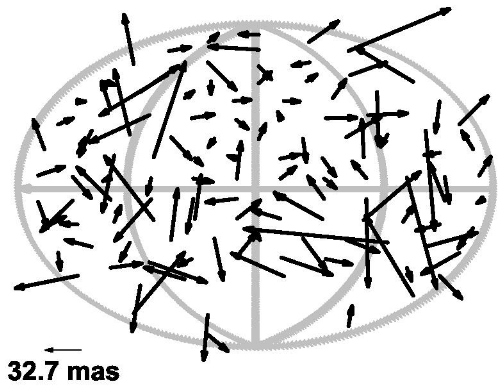

- average zonal errors of 32mas,
- average precision at 139mas.

- directly tied and
- compliant to the ICRF to 1.5mas

Morphology and the signature of the host galaxy

For AGNs in general, therefore also for QSOs, the host galaxy absolute magnitude should be brighter than -23.5. The host galaxy is thought of most of times be an elliptical or bulge dominated galaxy.

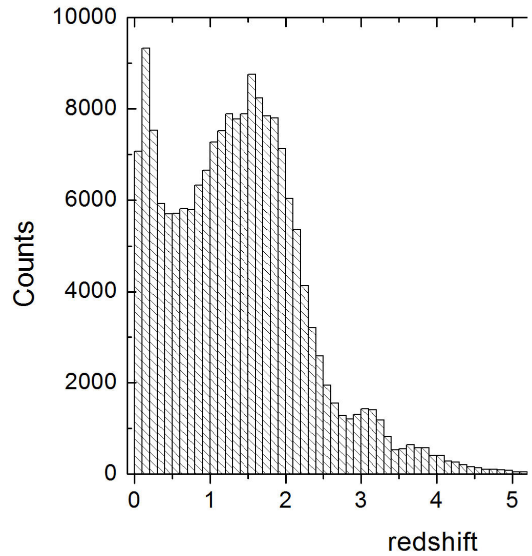

The host galaxy luminosity seems to increase proportionally to the strength of the central source, i.e. QSOs host galaxies may expected to usually be brighter than those around less powerful AGNs.

The size of the host galaxy also tends to follow the rule. Typical sizes for BLLac are 13kpc.

Host galaxies have regularly been resolved for AGNs to z < 1.5 and 1arcsec resolution. Less regularly so for QSOs.

The QSO space distribution peaks at z=0.6 for B=19, and at z=1 for for B=20.

That is, the largest fraction of Gaia QSOs would be of nearby ones.

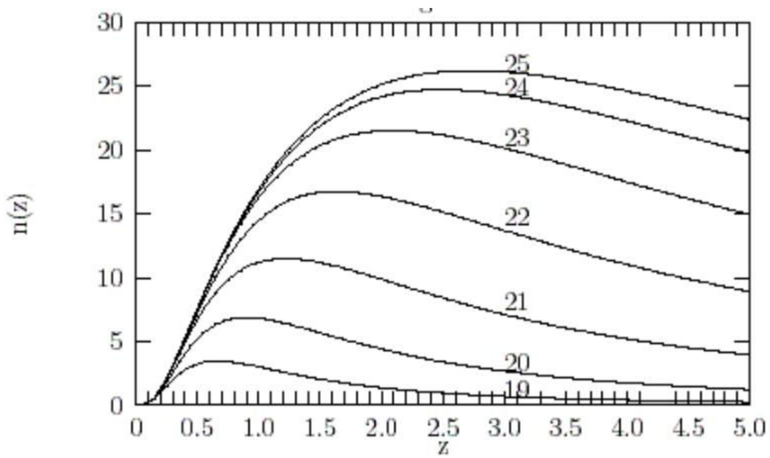

QSOs/deg^2 as function of redshift and magnitude (Crawford 1994)

Morphology and the signature of the host galaxy

One might expect a fair amount of contamination by alien AGNs among the Gaia extragalactic reference frame

(because they would look alike by the Gaia QSO selection criteria,

and because they still would look a lot pointlike).

One might expect a fair amount of resolved host galaxies around the Gaia extragalactic reference frame QSOs

(because the host galaxies do are large and bright enough,

because of contamination by alien AGNs,

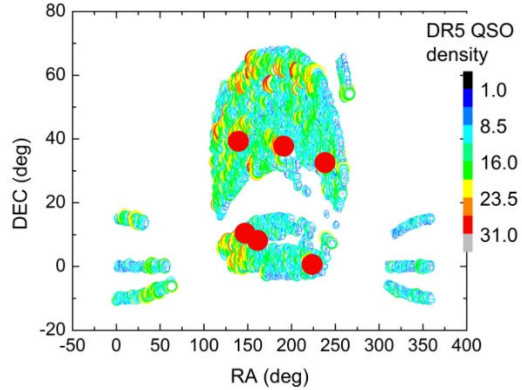

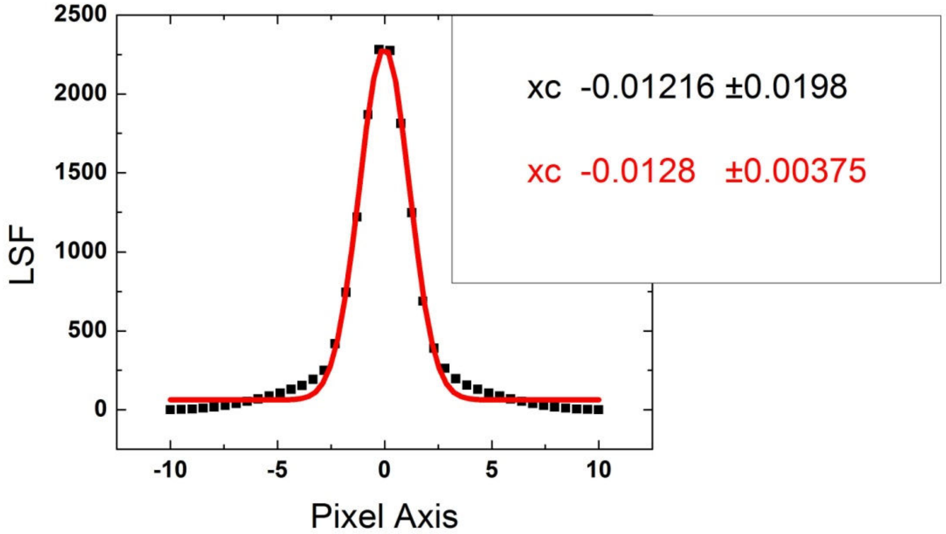

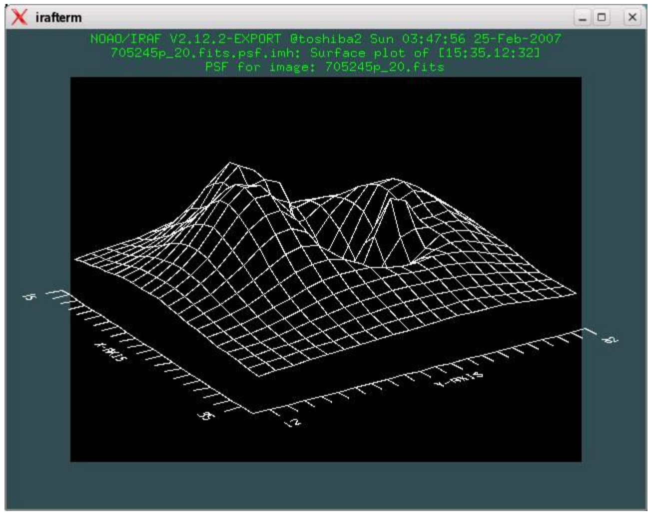

Morphology and the signature of the host galaxy

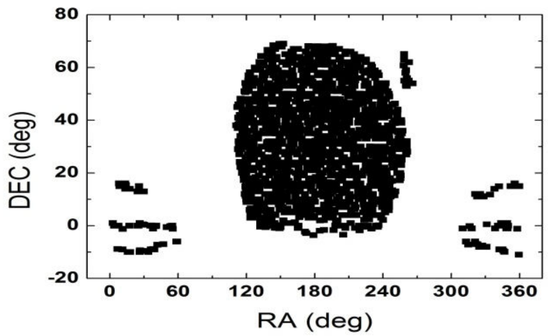

Trial bench on 1,343 DSS2 R images for which also the SDSS DR7 images (0.396arcsec/px) were retrieved. Extreme magnitudes, colors and redshift stored, along with a representative DR7 sky distribution.
Results show that a PSF (through IRAF's DAOPHOT) analysis reproduces well the SDSS star/galaxy separator – and that the DSS plates perform much alike to the SDSS frames.
The excess (*rate of objects beyond 2σ*) of non-stellar quasars is significant as given by all the indicators, on both the DSS2 and DR7 images, measured either against the field stars or the SDSS classified stars.

Object	$SHARP_{field}$	$SROUND_{field}$	$GROUND_{field}$	$SHARP_{class}$	$SROUND_{class}$	$GROUND_{class}$
QSO (DSS2)	0.19	0.31	0.43	0.55	0.23	0.33
QSO (DR7)	0.13	0.39	0.41	0.27	0.32	0.36
STARall	0.01	0.01	0.01	0.02	0.01	0.00
$STAR_{\Delta M=1}$	0.01	0.01	0.00	0.02	0.01	0.00

On basis of these results, we recovered all QSOs (from the previous version of the catalog) from the B, R, I available DSS images. The cuts are 5×5 arcmin. To assess the PSF we use SHARP (probing skewness), SROUND (probing roundness), and GROUND (probing normalness).

Morphology and the signature of the host galaxy

DSS color	N QSO	N	sharp sround ground	> 2σ
		SHARP	SROUND	GROUND
B	81,052	1,763	2,049	1,488
R	141,159	4,159	4,988	4,014
I	99,832	4,858	6,745	6,593

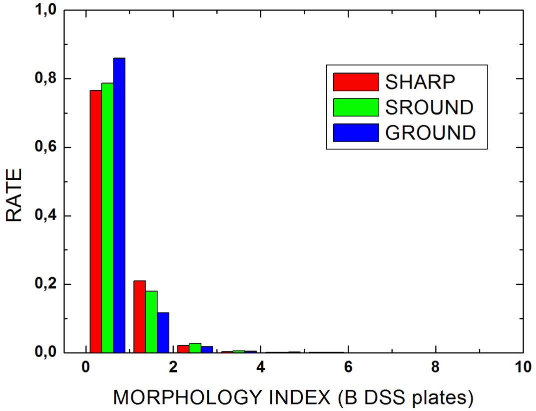

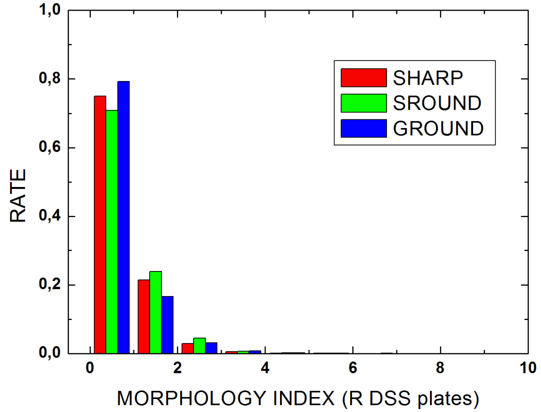

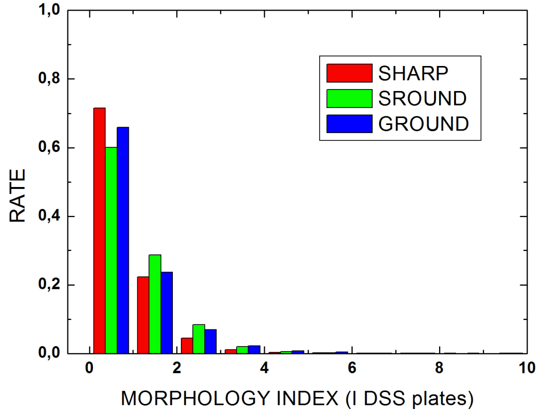

- ♠ As expected QSOs are very much pointilike. However, much similarly to the SDSS field test bench, more than 10% are not quite so, and more than 3% are far from it.
- ♠ The nonconformity is more evident for sharpness though the Gaussian nature of the PSF is not so affected.
- ♠ The results holding for the DSS2-DR7 images hold well on the entire sky basis.
- ♠ **These estimators are now included in the Gaia QSO Initial Catalog – for 145,505 sources (77.61/% of the catalog)**

Morphology and the signature of the host galaxy

- ♠ Taking the preceding plots and zooming into the region of non-pointlikeness.

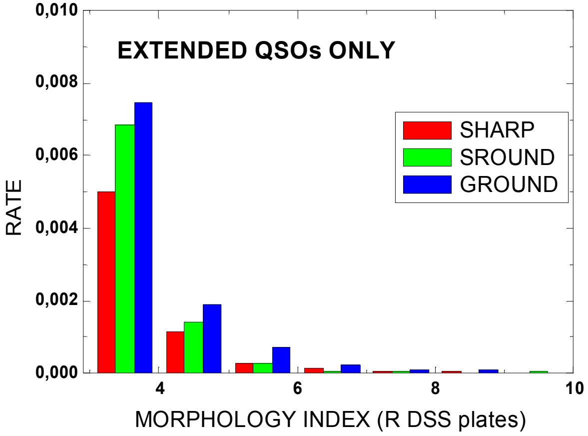

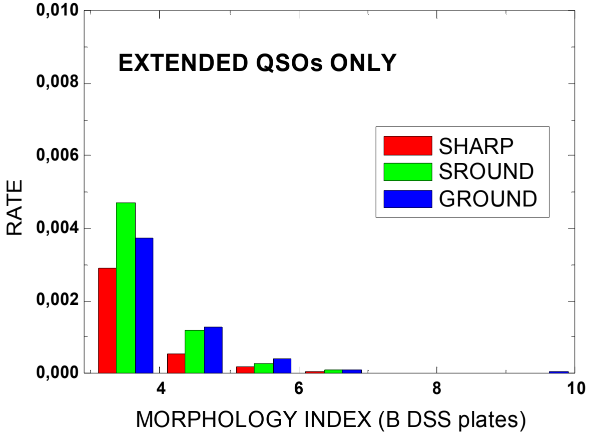

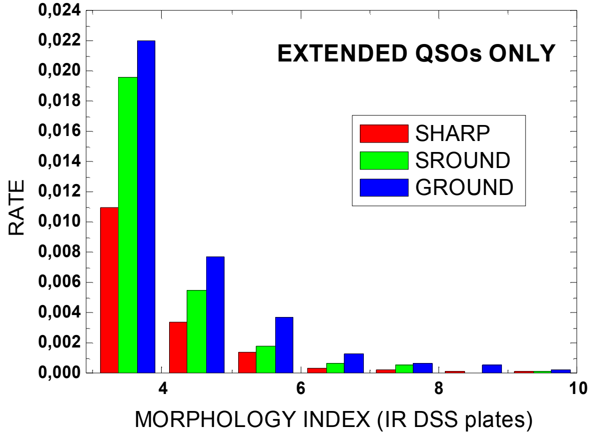

- ♠ It is evident that the degree of non-pointlikeness varies along the spectrum.
- ♠ The bluer the QSO is looked to, the deeper into the power force it is perused, and more pointlike it looks. (notice that the atmosphere transparency works right against this).
- ♠ The image treatment may accordingly be more or less complex along the spectrum, with useful results both for the astrometry and the interpretation.

♠ **Currently this morphological study is being applied to the complete of of ugriz images of the 105,783 SDSS QSOs (2 Tb!)**

Photometric and Astrometric Variability

One of the most important constraints on the structure of quasars is variability. It must assuredly be linked to some degree of motion of the photocenter. The demands of accuracy for the objects forming the fundamental astrometric frame of Gaia make mandatory a larger comprehension about the astrometric wandering of the photocenter and ìndeed a deeper comprehension of the mechanisms giving rise to optical emission in quasars.

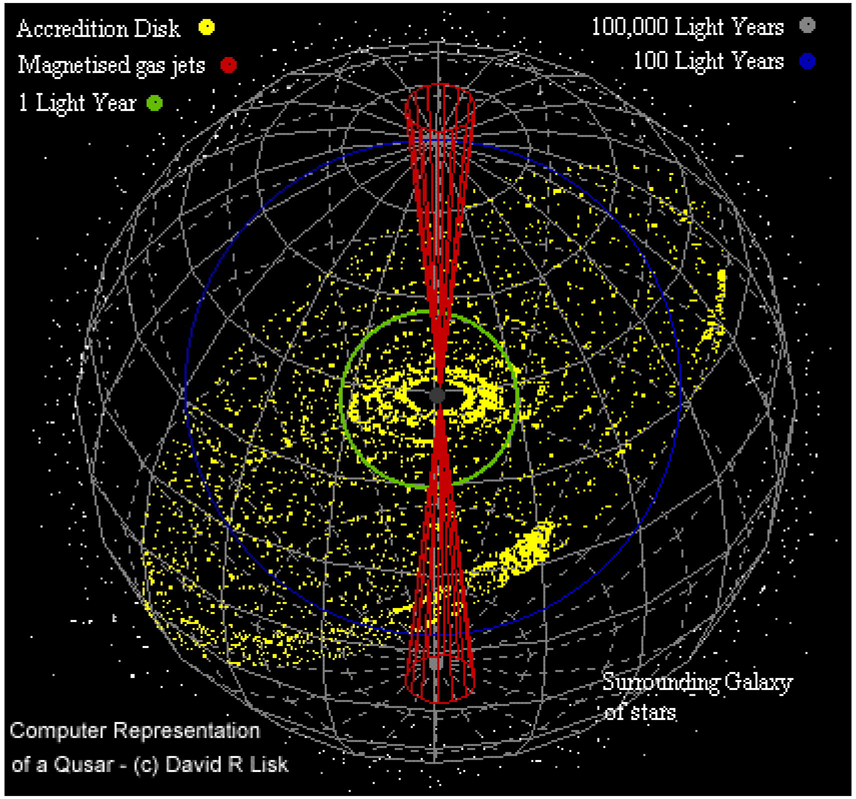

Since long, year/month-like, and large amplitude variations are also recorded, the sstandard reasoning itself would suggest that the other quasar's elements aren't at a stand-still.

There are several mechanisms apt to generate the optical and positional variability. **Opacity changes off the core regions; instabilities propagated from the accretion disk; emission from a precessing/disturbed jet; variability powered by a series of supernovae explosions; conversely variability triggered by stellar masses plunged towards the accretion disk; emission from regions at superluminal speeds; luminosity disturbance brought by the host galaxy; microlensing.**

Photometric and Astrometric Variability

r X10 for QSOs !

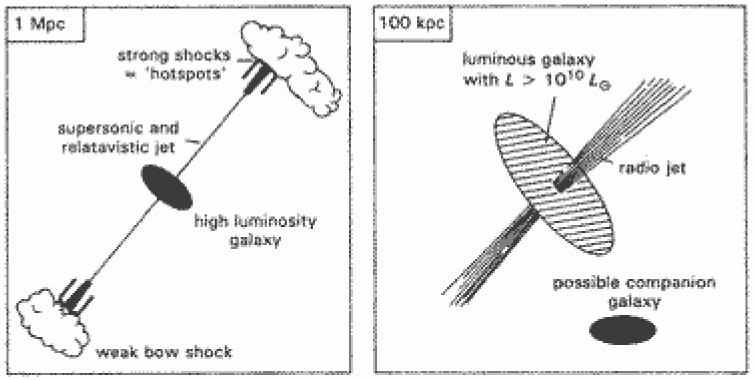

Extended radio sources — shown is an FRII source with an edge-brightened structure. The FRIs have lower jet velocities and fade-out to the ends.

The host galaxy. Although shown as an early type galaxy with a smooth profile, it could also be highly irregular with multiple nuclei as a result of merging.

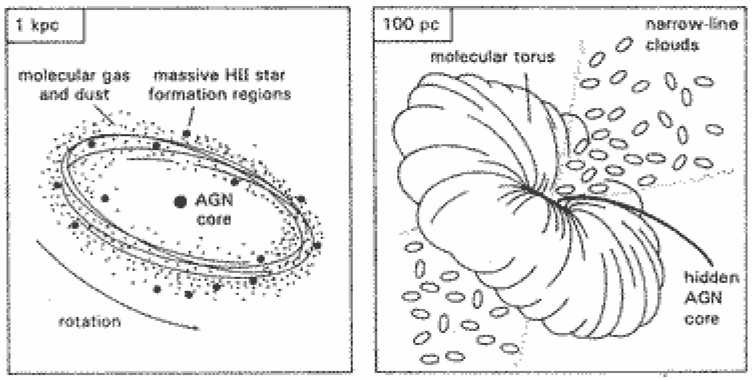

The central kpc star formation disk. This strong far infrared emitting zone might be fed by a bar structure, as seems to be the case for NGC1068.

The narrow-line region comprising small but numerous clouds of the interstellar medium ionized by the central AGN core.

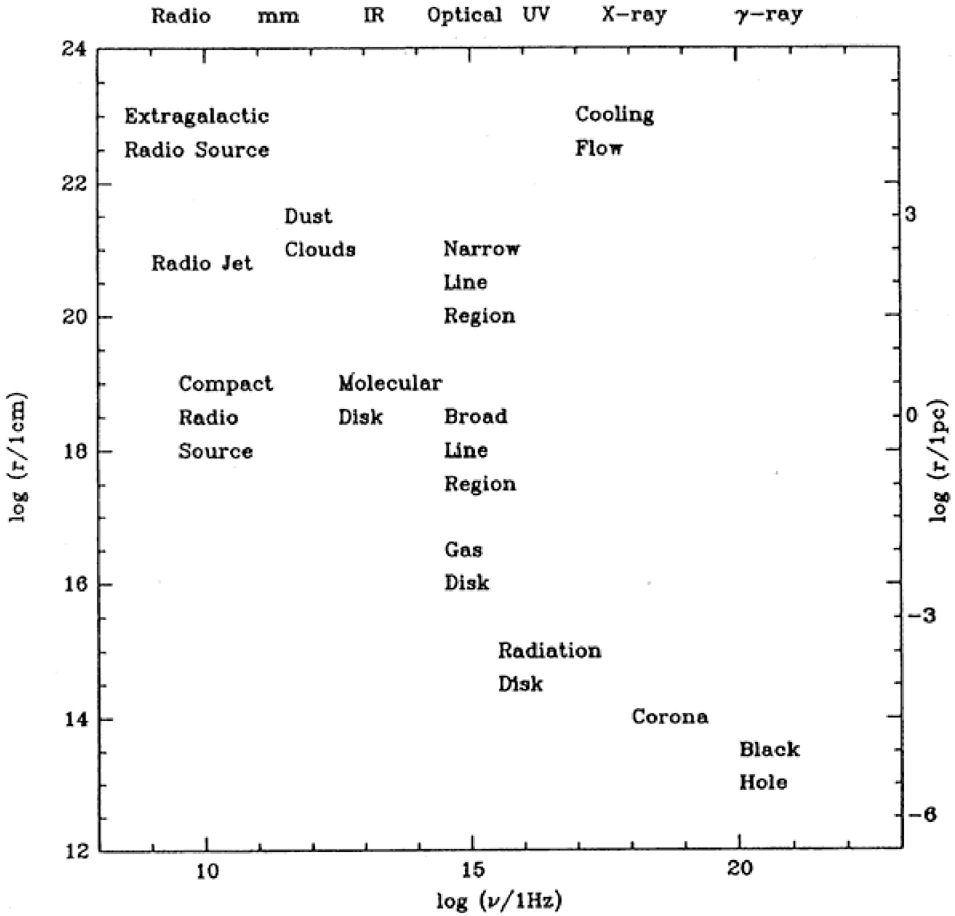

Fig. 1.1. Schematic illustration of the range of activity associated with the nuclei of galaxies. Phenomena have been observed spanning the full dynamic range of ~ 45 octaves of length scale from variable X-ray emission in Seyferts ($\lesssim 10^{12}$cm) to giant double radio sources ($\gtrsim 10^{25}$cm) and from metre wavelengths (low frequency variability) to 100MeV observations of some quasars and Seyfert galaxies (45 octaves of frequency). Some of these phenomena, *e.g.* radio jets, are observed directly. Others, *e.g.* accretion disk coronae and black holes are inferred indirectly and are of more questionable reality.

(*credit Bradford's SAAS Fee 1990 lectures*)

Photometric and Astrometric Variability - the ESO2p2 program

– **Observations** at the ESO Max Planck 2.2m telescope, La Silla, Chile, f8, 0”.238/pixel, WFI 4x2 CCD mosaic, on CCD 7 nearby the optical axis.

– Filters Rc/162 (peak 651.7nm, FWHM 162.2nm) and BB#B/123 (peak 451.1nm, FWHM 135.5nm). In each filter 3 frames are taken, to a combined SNR of 1000 (up to 2h total integration time). From April 2007 (P11) to July 2009 (P51) – largest interval 3months. Two final slots on Dec. 2009 and Feb./March 2010.

RA	DEC	Mag	z	P11	P12	P13	P21	P22	P23	P31	P32	P33	P41	P42	P43	P51
02:10:46.200	-51:01:01.89	16.9	1.003			3	1	1				1	1	1		
03:39:30.938	-01:46:35.80	18.4	0.852			1		1	1			1	1	1		
04:07:48.431	-12:11:36.66	15.3	0.574					1	1				1	1	1	
04:17:16.780	-05:53:45.50	15.9	0.781					1					1	1	1	
04:42:38.661	-00:17:43.42	19.2	0.850					1	1				1	1	1	
04:56:08.930	-21:59:09.50	16.1	0.534					1					1	1	1	
05:22:34.426	-61:07:57.13	18.1	1.400			1		1	1	1		1	1	1	1	
05:38:43.500	-44:05:05.00	17.5	0.894			1	2	1	1	1		1	1	1		
07:39:18.034	+01:37:04.62	16.5	0.191				1		1	1					1	1
08:13:53.020	+01:50:50.30	14.0	0.402					1		1					1	1
08:58:52.580	+16:51:27.20	17.7	1.048					1	1	1	1			1		1
09:09:10.092	+01:21:35.62	16.8	1.018												1	
09:25:07.270	+14:44:02.80	17.8	0.896					1		1				1		1
10:42:44.605	+12:03:31.26	17.8	1.029												1	1
12:18:55.810	+02:00:02.10	18.1	0.415					1	1	1	1			1		1
12:32:00.010	-02:24:00.80	18.7	1.038							1						1
12:54:38.256	+11:41:05.90	17.0	0.870							1	1				1	1
15:12:50.533	-09:05:59.83	16.9	0.361	1	1	1			1	1	1	1			1	1
16 20 11.290	+17 24 27.60	16.2	0.114	2	1				1	1	1	2			1	1
16 20 21.810	+17 36 24.00	17.4	0.555	2	1				1	1	1	2			1	1
17:51:32.819	+09:39:00.73	18.4	0.320	1	1	1			1	1	1	1			1	1

Variability elements from Teerkopi (2000, A&A 353,77). P ≥ 10y

Photometric and Astrometric Variability - the ESO2p2 program

Data Treatment:

- All images are treated by IRAF MSCRED for trimming, bias, flat, bad-pixel e split. Typically the image treatment enhances the SNR by a factor of 2.
- IRAF DAOFIND and PHOT are employed for the determination of centroids and (instrumental) magnitudes, with the entry parameters adjusted for each frame.
- Centroids and fluxes are obtained from the adjustment of bi-dimensional gaussians. The inner ring where the object counting is made and the outer ring where the sky background is counted are variable for each object and frame, but their ratio is kept constant.
- The plate scale and frame orientation are derived by IRAF IMCOORDS, from UCAC2 catalogue stars.
- The following tables bring the measures of precision (pixels).

N(tot)	E(x)	E(y)	E(M)
10229	0.017	0.017	0.001
24407	0.036	0.038	0.002

Average precision (1512-0905 sample). Upper row, best imaged objects. Lower row, all detected objects (above threshold 4)

N(R)	E(x)	E(y)	E(M)
7373	0.017	0.015	0.001
16527	0.034	0.034	0.002

N(B)	E(x)	E(y)	E(M)
2856	0.018	0.021	0.001
7880	0.038	0.047	0.001

Likewise for the R and B filters

Photometric and Astrometric Variability - the ESO2p2 program

at every step, independent third degree polynomes adjust (X,Y,M) to a common medium frame, using all common stars:

$$C_n^m - \langle C \rangle_n = C_0 + \sum_{i,j,k}^{1,3} A_{ijk}^m X^i Y^j M^k$$

Object **n** *of frame* **m**

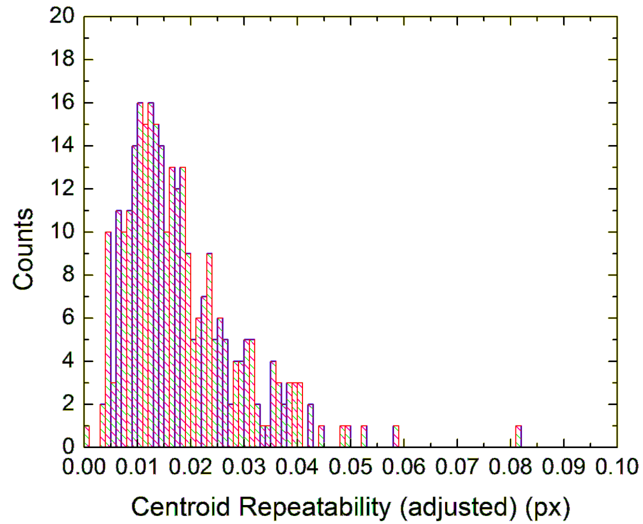

- 1st step: the night (usually 3) are adjusted to the average frame. The QSO position and magnitude is set to zero.
- 2nd step: the average frames from the different nights (i.e. Ppp) are sequentially adjusted to a super-average frame. The QSO position and magnitude is set to zero.
- 3rd step: from the super-average frame, common stars are picked up (if σ < 5 × -3 dex).
- 4th step: for each night, the sum of their (X,Y,M) residuals represents the QSO's variation respectively to the super-average frame.

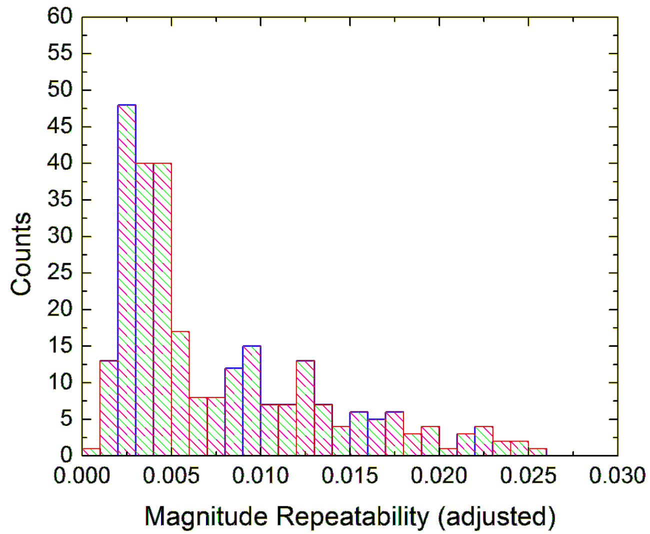

Photometric and Astrometric Variability - the ESO2p2 program

Results: **Time line - up to 435 days. There was always a preferred direction of the jitter. For 1512-0905 and 0522-6107 the preferred direction changed on time – but keeping strong autocorrelation. Nearby stars do not show such autocorrelation**

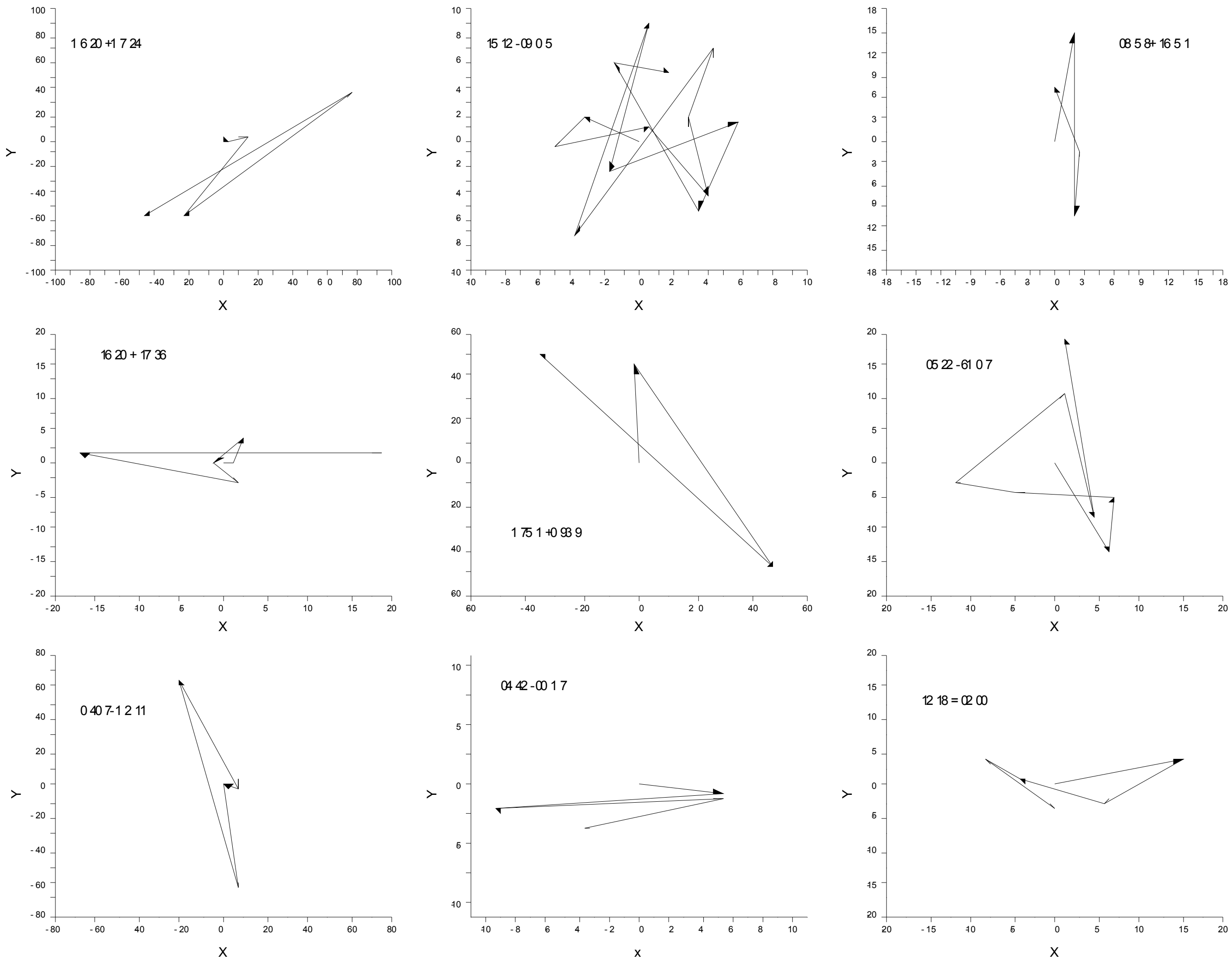

Photometric and Astrometric Variability - the ESO2p2 program

QSO	ΔX /ΔMag		ΔY /ΔMag		JitterX/ ΔMag		JitterY/ ΔMag	
	Pearson	Spearman	Pearson	Spearman	Pearson	Spearman	Pearson	Spearman
1512-0905	-0.42 (0.59)	-0.49 (0.33)	0.85 (0.00)	0.77 (0.33)	-0.80 (0.43)	-0.94 (0.00)	0.79 (0.00)	0.89 (0.02)
1620+1724	0.94 (0.00)	0.90 (0.04)	0.81 (0.01)	0.80 (0.10)	0.31 (0.48)	0.00 (1.00)	-0.30 (0.71)	-0.60 (0.28)
1620+1736	0.14 (0.76)	0.03 (0.96)	-0.52 (0.53)	0.09 (0.87)	0.38 (0.29)	0.31 (0.54)	-0.75 (0.44)	-0.49 (0.33)
1751+0939	0.58 (0.41)	0.50 (0.67)	-0.83 (0.73)	-0.50 (0.67)	0.96 (0.02)	1.00 (0.00)	0.62 (0.35)	0.50 (0.67)
0522-6107	0.44 (0.14)	0.46 (0.29)	-0.31 (0.62)	-0.32 (0.48)	0.22 (0.55)	0.36 (0.43)	0.15 (0.70)	0.14 (0.76)
0407-1211	-0.03 (0.97)	0.00 (1.00)	-0.12 (0.89)	-0.41 (0.60)	0.64 (0.13)	0.40 (0.60)	0.66 (0.11)	0.80 (0.20)
0442-0017	-0.46 (0.70)	-0.41 (0.60)	-0.40 (0.73)	-0.40 (0.60)	0.04 (0.96)	-0.80 (0.20)	0.40 (0.45)	0.40 (0.60)
0858+1651	-0.74 (0.61)	-0.20 (0.80)	-0.10 (0.91)	-0.20 (0.80)	-0.73 (0.61)	-0.20 (0.80)	-0.57 (0.66)	-0.80 (0.20)
1218+0200	0.03 (0.97)	0.20 (0.75)	-0.42 (0.64)	-0.50 (0.39)	-0.52 (0.59)	-0.70 (0.19)	-0.41 (0.65)	-0.30 (0.62)

Most, if not all, of the sources followed in the ESO2p2 program, exhibit from moderate to high correlation between the photocenter motion or jitter and the photometric variation. The astrometric variation is on average contained within 2mas, and presents excursions of 10mas. For redshift below z=1, this would imply either an outer jet component, or either the dust/molecular disks or the broad/narrow lines emission clouds.

Gaia will be sensitive to a region much closer to the quasar central engine, and should be much more sensitive to motions of the photocenter. The present study - variations from components off the accretion disk - indicates that an empiric modeling can be attempted, easing off the astrometric error budget.

Photometric and Astrometric Variability - the case of the nodding quasar

♣ 41 QSOs of the Deep 2 field were analyzed. QSOs images obtained during 4.5 years with the Canada France Hawaii Telescope (CFHT) in the frame of the CFHTLegacy Survey (CFHT-LS). All quasars showed variability, but the evidence of correlation is weak due the use of absolute astrometry.

♣ Relative PSF astrometry and photometry in the case of a QSO with a nearby star, evidentiates the correlation.

♣ CFHT image of the QSO 39436 with the nearby star (5” south). Correlation between the photocenter walk (green line) and the Blue and red magnitudes variation.

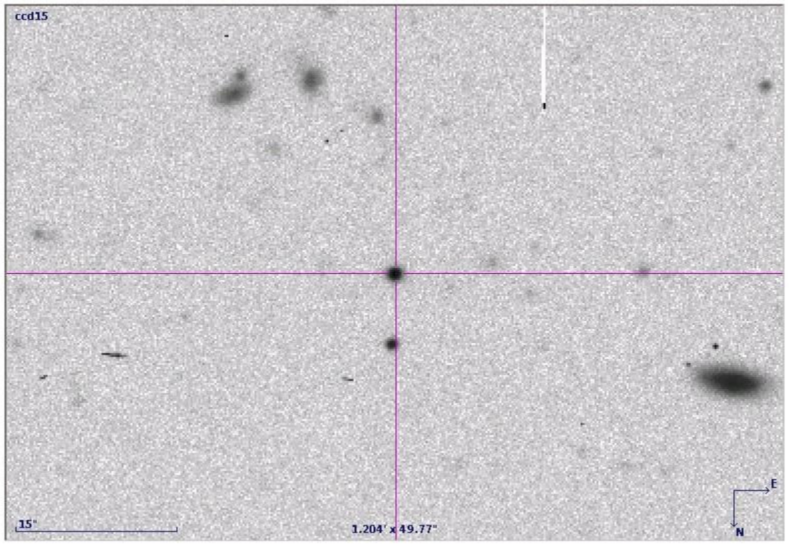

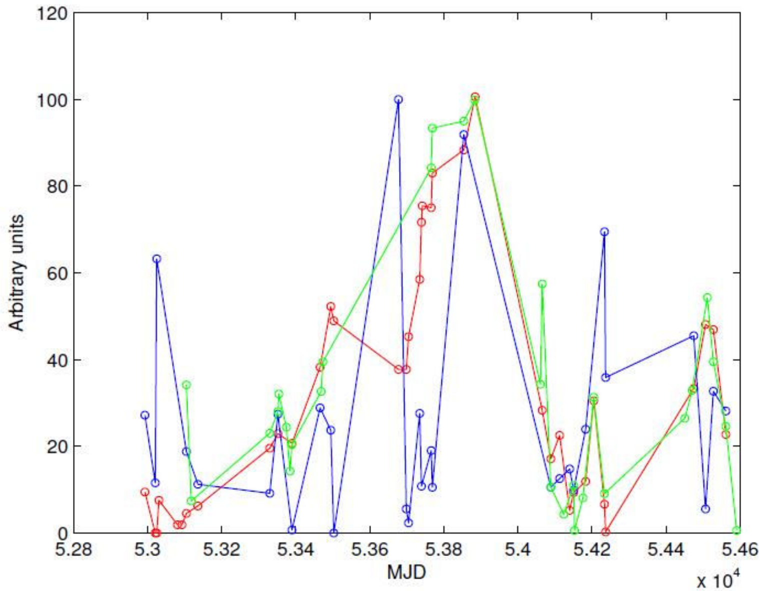

Photometric and Astrometric Variability - the CFHT/MEGACAM program

– **Observations** from the Deep Fields of the Legacy Survey.
– *g* , *r* , *i* filters, 1 deg^2 fields, 5y observations, 25 QSOs studied.

– Examples of the observed magnitude variation (time in months).

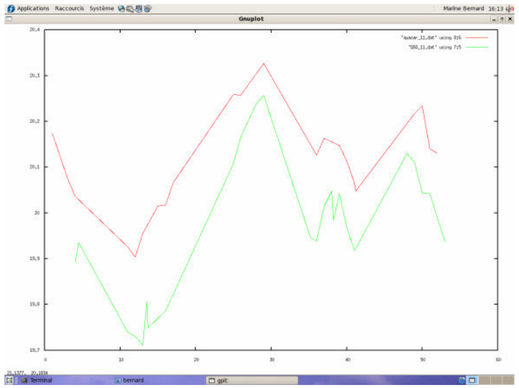
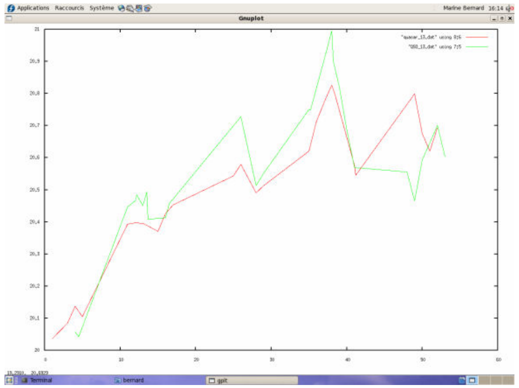
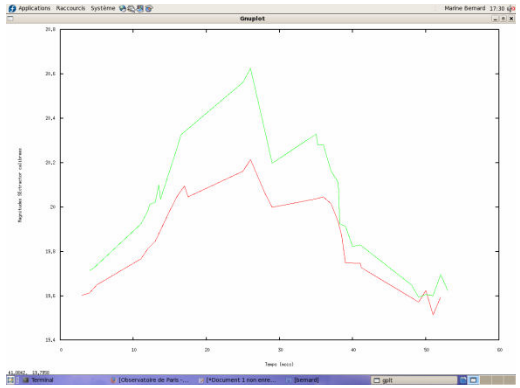
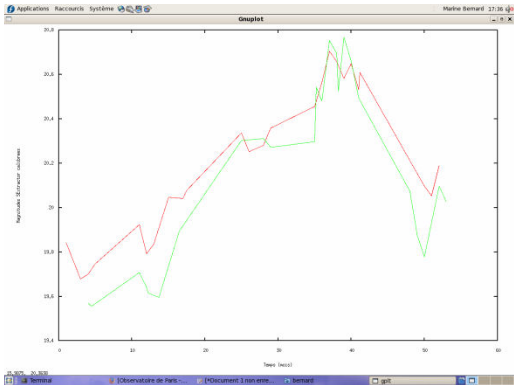
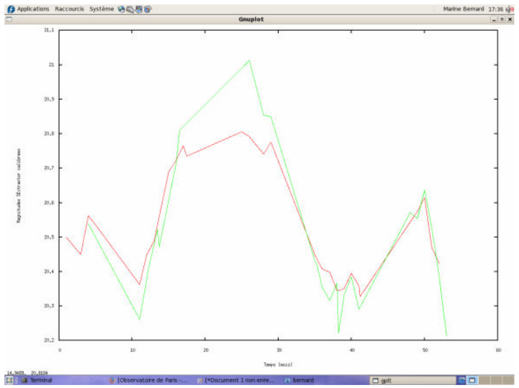
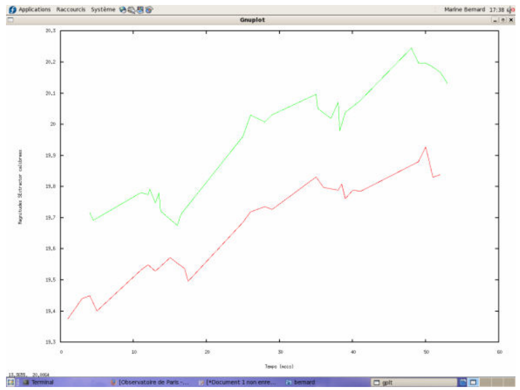

Photometric and Astrometric Variability - the OHP/1.2m program

– **Observations** at *T120 + CCD TK1024 OHP*. 48 QSOs brighter than V=18.

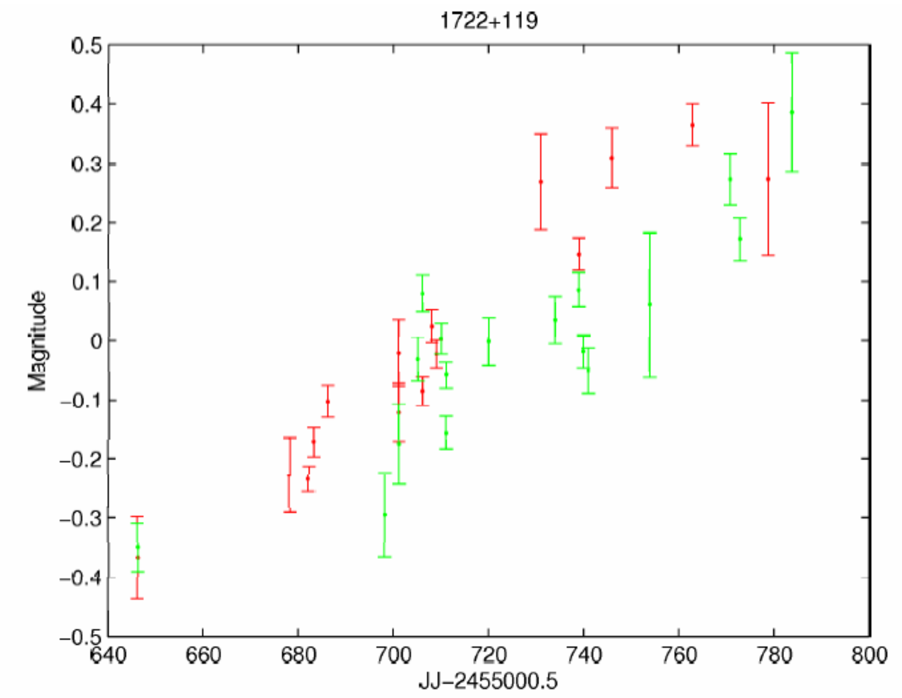

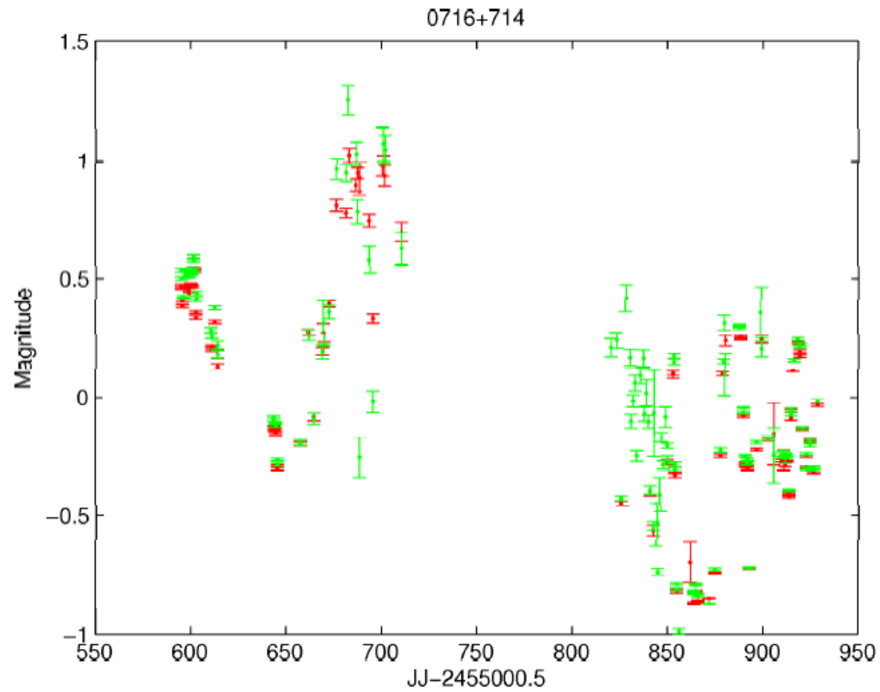

– **Dates obtained:** March 5th, 20th; April 5th, 18th; May 3rd, 14th; June 11th; July 1st, 16th; August 2nd, 13th **- service mode,**

Photometric and Astrometric Variability - Models

♣ Variability index based on Kelly et al. (2009) – V= A (Δt/y)$^{\gamma}$ to
(a) Ancillary quasar selection by on board measurements

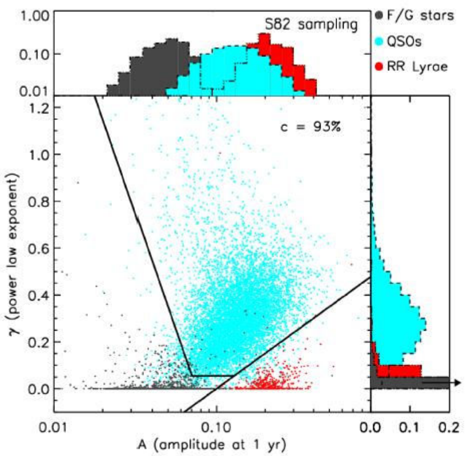

Distribution of the variability structure function parameters A and γ for 15,000 individual objects in Stripe 82. The spectroscopically confirmed quasars are shown as light blue points; confirmed RR Lyrae and color-selected F/G stars are shown in red and grey respectively. The three solid lines define the region in which the quasar completeness is 93%. Along the axes the projected A and γ distributions for the sub-samples is shown.

(b) Good separator from photometric contaminants

(c) Single out from the core objects for the construction of the fundamental Gaia frame or compensate the random walk on basis of the observed variability.

♣ A series of observational programs were started to bring experimental evidence, under extreme conditions (mas variations)

Photometric and Astrometric Variability - Models

- **Popovic et al. (2011) model** – Associated astrometric and photometric variability due to

(a) Instabilities in the accretion disk

M_{BH} $(M_\odot)$	z				
	0.01	0.05	0.10	0.15	0.20
10^8	0.036	0.007	0.004	0.003	0.002
10^9	0.355	0.074	0.039	0.028	0.022
10^{10}	3.550	0.744	0.394	0.278	0.220

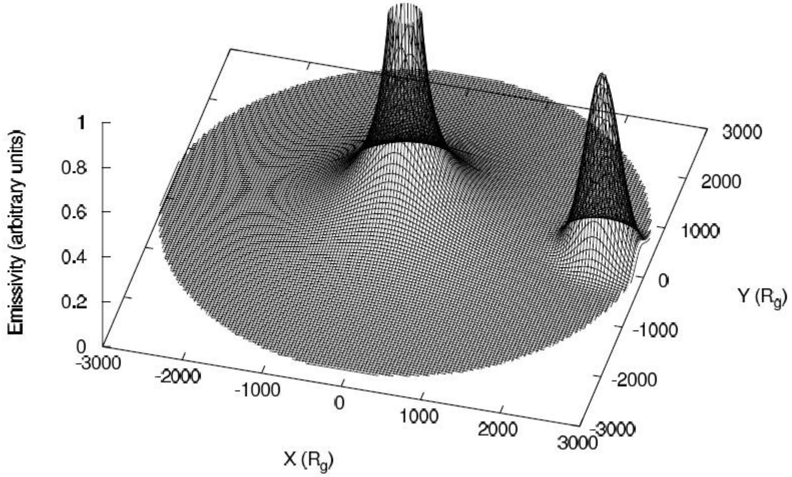

(b) density irregularities in the dusty torus

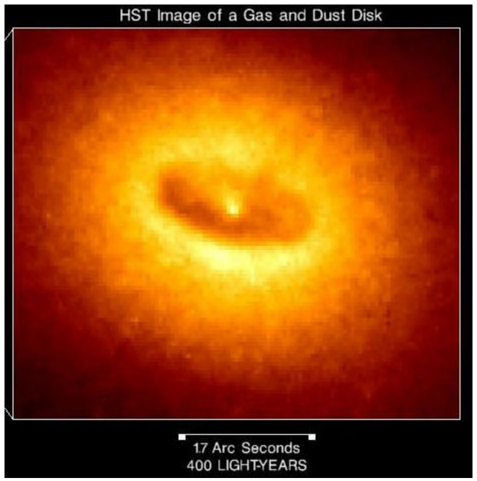

L $(10^{11} L_\odot)$	z		
	0.01	0.05	0.10
0.50 μm			
3	1.579	0.208	0.039
6	8.400	1.886	0.860
10	8.170	1.353	0.693

Photometric and Astrometric Variability – The Variability Index

♣ from z and V calculate Mabs (absolute magnitude) (Souchay et al, 2009)

♣ from Mabs calculate the QSO mass Mbh (Panov, 2011)

♣ from Mbh calculate the accretion disk radius (Morgan et al., 2011)

♣ from the Mabs scale up the accretion disk radius to calculate the dusty torus radius (Popovic et al., 2011)

♣ Now fully implemented in the GIQC IV

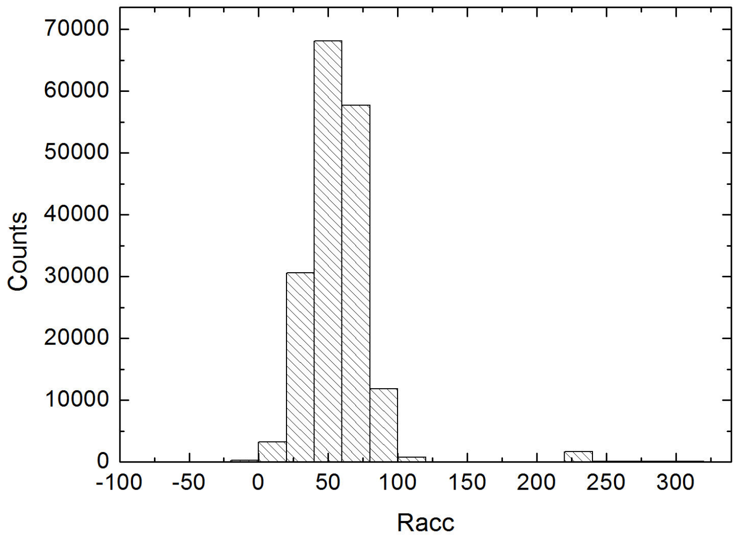

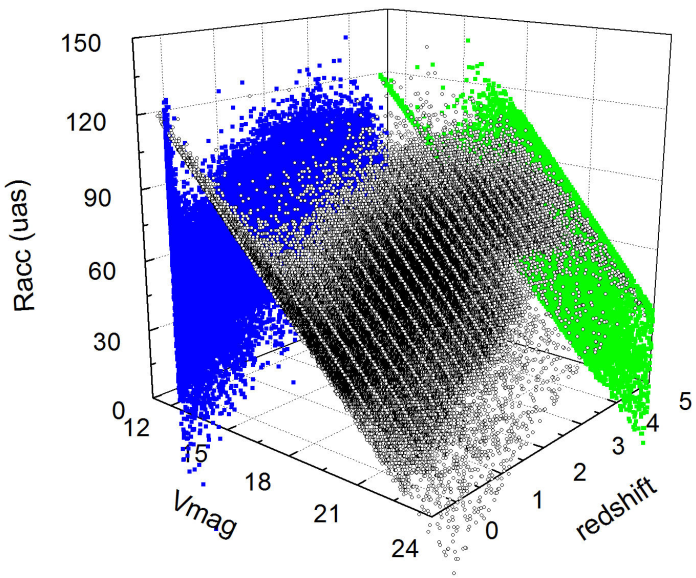

The Catalog – last week of version GIQC IV

RA (deg)	DEC (deg)	MAG	z	Rshr	Rsrn	Rgrn	Bshr	Bsrn	Bgrn	Ishr	Isrn	Igrn	AccDk	Torus	Class	
0.000000	-0.032778	19.40	1.560										59	5	C	P
0.002083	-0.450833	20.09	0.250										20	2	O	F
0.005291	-2.033269	19.29	1.356	0.75	0.10	0.13							56	5	D	
0.005735	-30.607458	19.18	1.143	0.20	0.01	0.91							52	5	D	
0.007326	-31.373790	19.74	1.331	0.73	0.44	0.00				1.82	1.14	1.37	50	5	D	
0.011279	-25.193609	21.56	1.314										29	2	O	F
0.012178	-35.059062	17.09	0.508	0.59	0.20	0.27				0.39	0.80	0.07	60	6	D	
0.022792	-27.419533	19.11	1.930	0.12	1.01	0.41							69	6	D	
0.027500	0.515278	20.37	1.823										52	5	D	S
0.033333	-63.593333	17.00	0.136										51	5	C	A
0.034167	0.276389	20.03	1.837										57	5	D	S
0.038604	15.298477	19.40	1.199	0.92	0.02	0.30	0.36	0.92	0.08	1.11	1.51	1.46	51	5	D	S
0.039089	13.938450	18.29	2.240	0.59	0.23	0.14	0.63	0.91	0.09	2.07	0.16	1.43	84	8	D	S
0.039167	23.954444	18.93	4.030										94	9	C	P

The table above brings the first lines of the present version of the GAIA Initial Quasar Catalogue - GIQC_IV

- RA and DEC are self-explanatory. And so is the redshift (z) on the 4th column.
- MAG is V whenever available. When it is not g, r, or the weighted average of the available colors.
- It follows 3 groups (from the DSS R, B, and I plates) of 3 PSF estimators (SHARP, SROUND, and GROUND) – for which the closer to 0, the more stellar-like is the QSO PSF (in the local photometric standard).
- Next, the Acrettion disk (μ as) and the Dusty Torus (mas) angular radii.
- The first Class column is - **D**efining, **C**andidate, or **O**ther
- The second Class column is -

SDSS source (for **D**s);
ICRF source, optically point-like **A**GN, or **P**oor observational history (for **C**s);
Empty field, low precision **R**adio position, **U**nreliable detection, or optically **F**aint (for **O**s)


Uffff! Ma tête!

Top Precision Astrometry

GAIA – galactic census, from 1 billion objects

– position, distance, motion

– multi-band photometry, broad-band spectroscopy

– reference frame as future paradigm of the ICRF (better than 1μas)

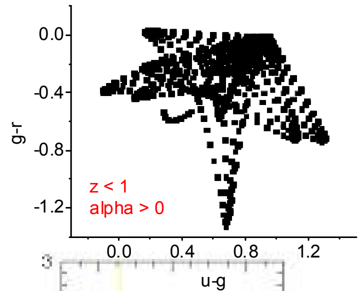

GAIA will observe ~ 500 000 QSOs to G< 20

Three independent methods based on GAIA data:

- photometry with ~ 15 passbands (color loci + templates)
- proper motions and parallaxes
- variability and morphology

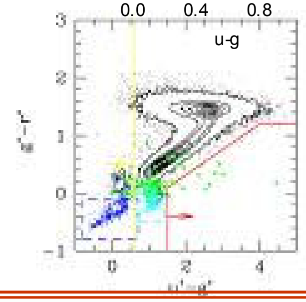

Two goals :

- complete survey allowing contaminants (classification)
- clean subsample with no contaminants

Major work on-going at the CU8 and CU3.

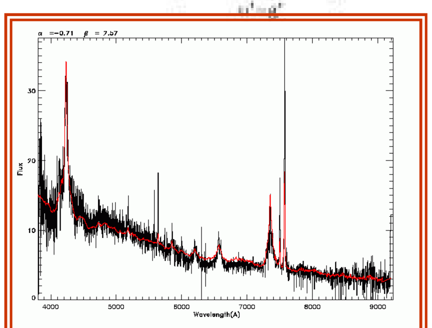

FIG. 2 – $z = 0.51, \alpha = -0.71, \beta = 2.57$